DOE/BC/14941-13
(OSTI_ID: 3257)

ADVANCED OIL RECOVERY TECHNOLOGIES FOR IMPROVED RECOVERY FROM SLOPE BASIN CLASTIC RESERVOIRS, NASH DRAW BRUSHY CANYON POOL, EDDY COUNTY, NM

Annual Report
October 1, 1997 – September 30, 1998

By
Mark B. Murphy

February, 1999

Work Performed Under Contract No. DE-FC22-95BC14941

Strata Production Company
Roswell, New Mexico

National Petroleum Technology Office
U. S. DEPARTMENT OF ENERGY
Tulsa, Oklahoma

DISCLAIMER

Portions of this document may be illegible in electronic image products. Images are produced from the best available original document.

DOE/BC/14941-13
Distribution Category UC-122

Advanced Oil Recovery Technologies for Improved Recovery from Slope Basin Clastic Reservoirs, Nash Draw Brushy Canyon Pool, Eddy County, NM

By
Mark B. Murphy

February 1999

Work Performed Under Contract No. DE-FC22-95BC14941

Prepared for
U.S. Department of Energy
Assistant Secretary for Fossil Energy

Dan Ferguson, Technology Manager
National Petroleum Technology Office
P.O. Box 3628
Tulsa, OK 74101

Prepared by
Strata Production Company
P.O. Box 1030
Roswell, NM 88202

TABLE OF CONTENTS

LIST OF TABLES

LIST OF FIGURES

ABSTRACT

Advanced reservoir characterization techniques are being used at the Nash Draw Brushy Canyon Pool project to develop reservoir management strategies for optimizing oil recovery from this Delaware reservoir. The reservoir characterization, geological modeling, 3-D seismic interpretation, and simulation studies have provided a detailed model of the Brushy Canyon zones. This model was used to predict the success of different reservoir management scenarios and to aid in determining the most favorable combination of targeted drilling, pressure maintenance, well stimulation, and well spacing to improve recovery from this reservoir.

The original Statement of Work included a pressure maintenance pilot project in a developed area of the field. The proposed pressure maintenance injection was not conducted because the pilot area was pressure depleted, and the seismic results suggest the pilot area is compartmentalized. Because reservoir discontinuities would reduce the effectiveness of any injection scheme, the pilot area will be reconsidered in a more continuous part of the reservoir if such areas can be located that have sufficient reservoir pressure.

Results from the project indicate that further development will be under playa lakes and potash areas that will be reached with combinations of deviated/horizontal wells. These areas are beyond the regions covered by well control, but are covered by the 3-D seismic survey that was obtained as part of the project.

EXECUTIVE SUMMARY

The Nash Draw Brushy Canyon Pool in Eddy County New Mexico is a field demonstration project in the U.S. Department of Energy Class III Program. Advanced reservoir characterization techniques are being used at the Nash Draw project to develop reservoir management strategies for optimizing oil recovery from this Delaware reservoir.

Reservoir simulation results obtained during the second year of the project suggested that the low permeabilities at the NDP will preclude waterflooding, but immiscible gas injection may be viable if initiated early and if undeveloped regions of the field can be found that have not been pressure depleted. During this third year of the project, reservoir simulation forecasts were extended to include both miscible and immiscible carbon dioxide injection. The forecasts suggest that areas of the field already under production may be candidates for CO_2 injection if pressures have not declined too much. However, a low-cost source of CO_2 is not currently available in the immediate vicinity of the NDP.

In the process of determining the feasibility of the pressure maintenance project, several problems were encountered: 1) as mentioned above, the relative permeabilities indicate that the permeability to water at the residual oil saturation may be too low to make water injection a practical method of pressure maintenance, 2) the seismic survey indicated that the area around the proposed pilot area is compartmentalized, and the individual zones are not always continuous between multiple wells, 3) analysis of the production data indicates that the compartmentalization, shown by the seismic results, is real, and 4) the reservoir pressure in the pilot area is very low. These problems indicated the prospect of success from the pilot pressure maintenance project was limited, and a more continuous area of the reservoir with less depletion would yield more favorable results. This resulted in a decision to shift the pressure maintenance pilot project into Phase II when new areas of the NDP are drilled.

Restricted surface access at the Nash Draw Pool, caused by proximity of underground potash mining and surface playa lakes, limits field development with conventional drilling. Further development will be under the playa lakes and potash areas that will be reached with combinations of deviated/horizontal wells.

The potential value of geostatistical techniques for estimating interwell reservoir properties, with infill drilling as a possible goal, was investigated. However, NDP wells primarily cover the center part of the available seismic survey, so a new technique was developed to extrapolate reservoir properties beyond the area directly constrained by wells. This new technique utilizes a nonlinear multivariable regression using seismic attributes as inputs and porosity, water saturation, and net pay as outputs. The regression equations allow the prediction of these three reservoir properties in areas without direct well control, and the resulting computed maps, such as hydrocarbon pore volume, will be used with other information to identify "sweet spots" for an aggressive development drilling program.

A plan for Phase II of the project has been submitted to the DOE, and the DOE has approved the continuation of the project into the next budget period.

INTRODUCTION

The Nash Draw Pool (NDP) in southeast New Mexico is one of the nine projects selected in 1995 by the U.S. Department of Energy (DOE) for participation in the Class III Reservoir Field Demonstration Program. Production at the NDP is from the Brushy Canyon formation, a low-permeability turbidite reservoir in the Delaware Mountain Group of Permian, Guadalupian age.

A challenge in developing these Delaware reservoirs of marginal quality is to distinguish oil-productive pay intervals from water-saturated, non-pay intervals. Additionally, because initial reservoir pressure is only slightly above bubble-point pressure, rapid oil decline rates and high gas/oil ratios are typically observed in the first year of primary production. Further, limited surface access, caused by underground potash mining and surface playa lakes at the NDP (see **Fig. 1**), prohibits development with conventional drilling in some parts of the reservoir.

The overall objective of this project is to demonstrate that a development program based on advanced reservoir management methods can significantly improve oil recovery. The initial demonstration plan included developing a control area using standard reservoir management techniques and comparing the performance of the control area with an area developed using advanced reservoir management methods. Specific goals to attain the objective are: (1) to demonstrate that a development drilling program and pressure maintenance program, based on advanced reservoir management methods, can significantly improve oil recovery compared with existing technology applications, and (2) to transfer the advanced methodologies to oil and gas producers in the Permian Basin and elsewhere in the U.S. oil and gas industry.

As proposed, this 5-year project had two budget periods; duration of the first budget period was two years and duration of the second budget period was three years. The first phase of the project was a "Science Phase" in which detailed reservoir characterization and project data, including the acquisition of 3-D seismic data, were to be analyzed to provide the basis for delineating appropriate reservoir management strategies. During Phase I, the feasibility of a pilot project was to be determined and the results of the pilot would be extrapolated to a full field implementation, if technically and economically feasible. Phase II of the project was the "Implementation Phase" in which results of the pilot testing would be considered for expansion to the remainder of the field. Because of delays in project initiation, evaluating new 3-D seismic data and reservoir complexities, and obtaining simulation software, the Phase I time frame was extended to three years, which resulted in a one-year, no-cost extension granted by the DOE.

During the first two years of the project, the Brushy Canyon reservoir at the NDP was found to be much more complex than initially indicated by conventional geological analysis. While the original concept pictured the NDP as a collection of thin channel sands continuously distributed between wells, the results from the Phase I work show the subzones within the sandstones are lenticular and are not always continuous from well to well. Although the original evaluation was that both the "K" and "L" sandstones were the major oil producing intervals, the results of this study show the primary oil productive zone at the NDP is the "L" sandstone.

The reservoir characterization, geological modeling, 3-D seismic interpretation, and simulation studies obtained in Phase I provided a more comprehensive model of the Brushy Canyon zones. A detailed reservoir model of the pilot area was developed, and enhanced recovery options, including waterflooding, lean gas, and carbon dioxide injection, were considered.

RESULTS AND DISCUSSION

This is the third annual progress report on the project. Results obtained in the first two years of the project are discussed in previous annual reports[1,2] and in technical papers.[3-9] Results obtained during this reporting period are summarized in this progress report.

Project Management

A Project Evaluation Report, plan for Phase II, statement of work, and Phase II budget was prepared and submitted in August 1998. Phase II is proposed to include directional/horizontal drilling and early pressure maintenance to develop reserves under surface-restricted areas and potash mines in order to enhance the ultimate recovery from the project.

Data and Databases

The production database was updated through August 1998. These data were added to the history of each well to update the decline curves and to project ultimate recoveries as well as to assess the effects of interference and production strategies.

Data are being compiled in response to the Technical Data Request made in February 1998. It is anticipated that the project data and TORIS data will be submitted at the conclusion of Budget Period I.

The test version of the Advanced Log Analysis program for predicting potential productive zones in Delaware reservoirs is being developed. After testing and verification, this program will be available for distribution.

Recent Seismic Interpretations

The basal Brushy Canyon sandstones are deposited on the top of Bone Spring depositional surface, which influences the quality of the reservoir and the continuity of the individual sands in the Brushy Canyon formation. To further understand the importance and the origin of the depositional surface for the basal Brushy Canyon sands at the NDP and enable the extrapolation of this information to other areas, a 10,000-foot interval from the Cherry Canyon to the Morrow formation was investigated. In addition to the seismic interpretations of the "K" and "L" pay intervals in the Brushy Canyon formation at the NDP, recent seismic interpretations have been extended to include the Morrow, Bone Spring, and Cherry Canyon formations.

3-D Seismic Interpretation of Morrow System

The position of the Morrow formation in the 3-D seismic data volume obtained in the NDP project was estimated by extending the time-vs-depth trend of the VSP data in NDP Well #25 to a depth of 13,000 ft, which is the assumed depth of the Morrow formation at the NDP. This assumed depth equates to a 3-D seismic image time of approximately 1.75 sec. Four sets of displays were prepared to describe the seismic interpretation of the Morrow system.

Initially the vertical profiles and time slices through the unflattened 3-D seismic data volume were reviewed. NDP Well #25, the VSP well, is located at trace coordinate 132 and line coordinate 58 (Landmark software notation) of the seismic image space. The vertical profiles follow these inline and crossline well coordinates. The position of the Morrow formation (**Fig. 2**) is shown as a tic mark on the section view. Inspection of the 3-D data showed that there was a reasonably continuous, good quality reflection peak approximately 30 ms above the calculated position of the Morrow formation. This overlying peak was interpreted across the complete data volume and was used as a reference surface for the Morrow interpretation. This reference surface is labeled 1710 ms horizon on the vertical section. There is evidence of Morrow faulting in this section view and in map views. The time slices pass through the assumed Morrow section. In these horizontal views, faults appear as linear disruptions in reflection amplitude.

The 3-D data were flattened on the 1710 ms reference horizon for the north-south profile 132 and east-west profile 58. Also on these vertical sections are two surfaces 20 ms and 50 ms below the 1710 ms reference surface that are conformable to the reference surface. The data window between these two surfaces spans the Morrow system. A number of time slices were cut through this Morrow-dominated data window to determine if any depositional patterns, such as stream channels, could be discerned. These time slices are reasonable approximations of Morrow-age stratal surfaces. No depositional patterns are obvious on these slices; however, fault trends are easier to see on these constant depositional-time surfaces than on the time slices through the unflattened data volume. North-south fault systems were identified, and each trend is manifested by a linear disruption in reflection amplitude.

Figure 3 is a time structure map of the 1710 ms horizon. This map will be assumed to be equivalent to a Morrow depth map until there is adequate well control and velocity control to modify the structural configuration. Various attributes were calculated over the 30-ms data window that spans the Morrow system. The attributes that were analyzed were maximum peak amplitude, maximum trough amplitude, energy half time, average instantaneous frequency, average reflection strength and the ratio of positive to negative amplitude. This data window is sufficiently narrow that any seismic attribute that reacts to Morrow deposition should reveal areal patterns of Morrow stratigraphy. No attribute shows a depositional pattern that is particularly intriguing. Almost every attribute shows some type of discontinuity that is related to the faults that have been described previously.

Reflector continuity at the Morrow level was analyzed. Changes in reflection continuity indicate faults and stratigraphic terminations such as pinchouts and channel boundaries. Linear fault trends were depicted rather well, but no depositional pattern occurs that would suggest the presence of a Morrow channel system.

3-D Seismic Interpretation of Bone Spring Formation

The Permian (Leonardian) Bone Spring Formation directly underlies the Brushy Canyon Formation (Guadalupian) in the Delaware Basin of SE New Mexico. Both units are thought to have been deposited in a deep water basin, and both are considered to be prospective drilling targets in various parts of the basin. As such, study of the Bone Spring formation should help to illuminate the controls on reservoir development and heterogeneity in the basal Brushy Canyon formation, both by identifying similarities in depositional processes and by helping to establish the structural framework of the Delaware Basin during Leonardian and early Guadalupian time. The NDP area provides an exceptional opportunity to study the influence of Leonardian structures on basal Brushy Canyon deposition and production. A vibroseis 3-D seismic survey and a vertical seismic profile (VSP) were available, as well as numerous digital logs that reach the top of the Bone Spring formation.

The structural and stratigraphic characteristics of the Bone Spring formation in the NDP area were examined. The database consisted of 3-D seismic data, well data, and sidewall core analyses. The log-based stratigraphy was tied to the seismic data via a synthetic seismogram that was generated for NDP Well #1. The tops of the Sand and Carbonate Members of the Bone Spring were then traced throughout the dataset. Structure maps of these seismic horizons generally show increasing structural complexity with depth. The principal structural trends tend to overlie one another. These observations suggest that the structural fabric up through the Bone Spring formation at the NDP was controlled largely by movement of deep-seated basement structures, and that this movement decreased throughout Bone Spring deposition. Some of the structure may be related to depositional processes as well.

Current practice in 3-D seismic analyses[10] dictates that 3-D seismic analyses need to be integrated with geologic and engineering data and concepts. No Bone Spring production data are available for the NDP area, but the current report integrates sequence stratigraphy, structural interpretations, log analyses, sidewall core analyses, seismic modeling, and attribute analyses. Many of the interpretations presented herein, are of a qualitative nature. This is a function of: a) the "exploration" nature of the investigations, and b) the relative lack of digital data that would permit numerical treatments for much of the Bone Spring interval.

The Leonardian (Permian) Bone Spring formation of New Mexico records a well-defined transition from slope to basin floor deposits. These rocks were primarily deposited by slope and deep water resedimentation of carbonate and clastic detritus supplied from carbonate-dominated platforms around the periphery of the Delaware Basin (e.g., Reference 11). The formation is divided into thick, carbonate and clastic ("sand"), members that reflect the history of relative sea level change within the basin. Current sequence stratigraphic models[12] suggest that the siliciclastic sediments were delivered to the basin during relative sea level lowstands.

Reservoirs in the Bone Spring are the product of complex interactions between depositional processes, diagenesis and subtle structural deformation. Production, including oil and gas from both carbonate and sand members, has traditionally been mostly from a "fairway" within 5-15 miles of

the shelf edge. Within the past few years however, other fields are currently being discovered and produced in basinal areas further south in more basinal areas (see Fig. 1 in Reference 13). These basinal fields typically have production from the sandstones (e.g., Old Milliman Ranch - 1st Sandstone, Red Hills - 3rd Sand, Sand Dunes South - Avalon Sand). Little has been published[13,14] on these plays.

Most of the database for this study was provided by the Texas Bureau of Economic Geology (BEG) on two 8 mm tapes. These tapes had backups of the Landmark "OpenWorks" (well logs, log picks, geographic information) and "SeisWorks" (seismic data, seismic horizons) projects that had been used for their study of the basal Brushy Canyon. Additionally, Pecos Petroleum Engineering provided sidewall core porosity and permeability analysis measurements (from the Bone Spring Avalon Sand) as well as digital logs for NDP Wells #29 and #38. None of the logs from any of the wells penetrated through the entire Bone Spring formation. Therefore, the gamma ray and sonic logs from NDP Well #1 were digitized from a paper log archived at the New Mexico Bureau of Mines and Mineral Resources to a depth of 13,850 ft. Most of the wells in the study area penetrated only the upper few hundred feet of the Bone Spring formation. Other than the newly digitized logs from NDP Well #1, only NDP Well #20 had logs that penetrated more than this, going a little over 1300 ft into the formation.

Time-depth information from the VSP test was available for NDP Well #25. Unfortunately, this highly accurate data only provided information into the uppermost part of the Bone Spring interval. In an attempt to make the tie between time and depth for the lower part of the formation, time-depth (check shot) surveys for two wells in this part of the basin were entered into the OpenWorks database: 1) Remuda Basin #1, Section 24 23S 29E, and 2) Poker Lake #11, Section 28, T24S-R31 E.

The 3-D seismic dataset was examined to investigate data quality and how much of an acquisition footprint was present. The acquisition footprint is that part of the seismic data that is related to the way the data were acquired and processed, rather than to subsurface geology. Transects through the data volume were reviewed. A "mottled" appearance was observed in the reflections in the middle of the transect, and a "blurred" appearance was observed in the data along the edges of the transect. The latter effect is common along the margins of seismic surveys and results in decreased amplitudes and picks that are deleteriously affected by unwanted artifacts. As such, the margins of structure maps and attributes (and their derived products) from the margins of the data should be treated with suspicion. The mottled appearance can be removed in part by "dip filtering" the data, and the "noise" was rejected by dip filtering the data using Landmark's PostStack application. However, in addition to the unwanted high-angle dipping events, some signal (horizontal reflections) was unfortunately removed. Some mottling is still present, but tests showed that more aggressive filter application removed too much of the wanted signal in the data (less aggressive filtering did not remove enough of the unwanted high angle events). The dip filtering process can help clean up the data before conducting attribute studies[15], and all attributes used in the Avalon Sand study (see below) were extracted from the filtered dataset.

One of the key components of any seismic study is making the link between the seismic

response and the geology as observed in wellbores. The VSP results allowed the ties to be made with great precision for the interval down to the top of the Bone Spring formation, but did not go deep enough to show the expected response of all members of that unit. As such, it was necessary to tie the wells and the seismic by generating a synthetic seismogram.

The digitized sonic log for NDP Well #1 was used for generating the synthetic seismogram (no density log was available to help improve the tie). Several synthetics were generated using different wavelets, and the best result was generated by using wavelets that were extracted from the seismic data using Landmark's Syntool application.

The apparent tie is not very good at the top of the Bone Spring (although the VSP shows that the strong peak is the top of the formation) but the ties for the remainder of the section are good. This synthetic shows that the tops of the Carbonate Members are characterized by slow to fast transitions that are represented in the seismic data by peaks. Conversely, the tops of the Sand Members, fast to slow, are represented by troughs. The poor tie at the Bone Spring level can be explained either by: a) problems with the sonic log at that level, or b) velocity problems that arise when the software changes from the time-depth information from the VSP to one created from the sonic log. By integrating the sonic log, Syntool's synthetic generation process creates a time-depth table that can be used to tie the well to the seismic data in SeisWorks The time-depth table so generated gave a much better tie between the well and seismic data than either of the checkshot surveys that had been entered.

The synthetic from NDP Well #1 was used to help determine which seismic reflections correspond to the tops of the various members in the seismic data. For some picks the choice of which reflection (peak/trough) to begin picking was clear, whereas for others the choice remained somewhat ambiguous, even given the relatively good tie between the seismic and the synthetic. In these latter cases, other criteria were employed. For example, the reflections corresponding to Member tops should be relatively continuous throughout the survey area (since the Members are continuous throughout the Delaware Basin). Additionally, certain expected sequence stratigraphic geometries (downlap, toplap, etc.) were looked for at each level. Some of the selected seismic reflections were continuous throughout the area; others appeared to be at least locally discontinuous. Having another "deep" well in the survey area with a synthetic would have allowed the picks to be checked, adding another degree of confidence to the process. Without such a well, the best approach was to attempt to ensure the integrity of the picks by boxing them in using a grid of picked lines and thus making sure that interpretations for each horizon are internally consistent.

Time structure maps for the Bone Spring horizons were generated with 2 ms contour intervals. These maps were generated by exporting the seismic picks into the Z-Map + mapping package. In that package the picks were gridded and then contoured. The gridding processes filters ("smoothes") the result somewhat.

The top of the Bone Spring formation is represented by a high amplitude peak with approximately 20 ms of relief, ranging from about 978 - 998 ms (**Fig. 4**). The pick is highest in the west and has 2 low areas, the first of which is more or less N-S and runs through the eastern part of

Sections 11 and 14. The second low is approximately NE-SW going from Section 7 to Section 13.

The origins of the subtle structural features of the Bone Spring formation at the NDP are probably multiple. The observations indicate that the same structural trends that are observed at the top of the Bone Spring horizon are present, but accentuated, at the level of an unidentified seismic reflection at approximately 1500 ms TWT (two-way travel time). However the trends are not present at the level of an unidentified seismic reflection at approximately 300 ms TWT. These observations, and examination of the time structure maps from the Bone Spring, suggest that structuring that might be associated with deformation generally increases with depth in this area.

It is believed that the main structures at the Bone Spring level in this area are the expression of subtle relative movement on basement blocks during the Permian period. Initiation of structure development began in the Pennsylvanian period, a time of tectonic activity during which the Central Basin Platform was raised. Tectonic activity, including reactivation of basement features, was probably less intense in the NDP area because it is relatively far removed from the deformation front. Structure development continued but decreased during the Permian period, so that, by the end of the Leonardian series (top of Bone Spring) and into the early Guadalupian series (lower Brushy Canyon), subtle structures continued to influence depositional patterns.

A second possible origin for some of the structures relates to depositional features. Channel sands are known to represent "highs" in basinal deposits of the Delaware and Midland Basins (Delaware Mountain Group, Wolfcamp and possibly Bone Spring). The highs are the product of differential compaction-sand-filled channels that were once depositional lows which were compacted less than the surrounding finer grained deposits, and thus became features with a positive relief. Convex up profiles (positive relief) are seen locally at the top of the Sand Members, suggesting that channel sands may be present. In the absence of well control, the channel interpretation would need to be tested through seismic modeling that is based on analogous deposits.

A third possible origin for some of the structures relates to velocity artifacts (e.g., velocity pull-up or push-down). Examination of the migration velocity cube, provided by the BEG, shows some lateral variability in migration velocities in the Bone Spring interval. Further work would be needed to assess this possibility.

The top of the Bone Spring formation is well defined in NDP Well #24. Bone Spring limestones are identified by GR = 30 API, RHOB = 2.71 gcm^3, PEF = 5, and DT = 50 µs/ft. The Avalon Sand is identified in this well as a unit extending from 6995 ft to 7062 ft, with GR = 55 API, RHOB = 2.5 gcm^3, PEF = 2, and DT = 60 µs/ft. Although sonic logs are not available for all wells in this area, GR, PEF and DPHI logs for intervals covering the Avalon Sand are available for 12 wells. As such, the thickness of the part of the Avalon with DPHI > 12% could be derived.

Simultaneous examination of the 3-D seismic and log data from the NDP indicates that the Avalon Sand is detectable in the seismic as a discontinuous peak approximately 16 ms below the Bone Spring seismic pick. This conclusion is supported by the results of the seismic modeling at Sand Dunes South which showed that the Avalon sand should be identifiable as a seismic event

approximately this distance below the Bone Spring pick.

Unfortunately, because the peak is not continuous, it is not possible to directly pick the horizon in the seismic data. As such, the best method for creating an Avalon horizon for the NDP survey was to create a horizon that is 16 ms TWT below the Bone Spring pick. Examination of this horizon shows that it generally, but not everywhere, corresponds directly to the Avalon peak.

Seismic attributes were explored as a means of predicting the thickness of the Avalon Sand throughout the Nash Draw 3-D seismic coverage. Since the Avalon seismic pick could not *exactly* track the horizon, it was decided that "instantaneous" attribute measurements would not be meaningful. Instead, "average" attributes were derived for a "window" that extended 6 ms above and below the horizon. Isochron ("thickness") measurements were not considered to be useful, given the way that the horizon was generated. Furthermore, some further judgment calls (based on previous experience and the results of the seismic modeling at Sand Dunes South) were made during the attribute generation process to further reduce the number of attributes that would need to be generated for the study. In the end, more than 40 attributes were examined in an effort to establish relationships with the log based measurements. These attributes were extracted from the filtered data set, since it is known that suppression of the acquisition footprint should help during the attribute calibration process.[15]

Spearman'sRank coefficient was used to determine which attributes had the best correlation (not necessarily a linear relationship) to the "porosity thickness" (PT) log property. The 3 highest ranking attributes were used alone and in various combinations for multivariate regression analyses. The best result was obtained for a second order regression that uses: a) average absolute amplitude (x), b) average reflection strength (y), and c) root mean squared amplitude (z) for the analysis window. The equation is:

$$PT = 171.505 + 11.0805x - 0.0957246x^2 - 1.46759y + 0.0108395y^2 - 13.5454z + 0.1\,07737z^2$$

The standard error for the relationship is 3.7. The coefficient of determination, or how much of the variation in PT is explained by this combination of attributes (0 = none, 1 = all), is 0.84. Equally significant to the high coefficient of determination is that all three of the highest ranking attributes are related to amplitude (reflection strength is amplitude independent of phase). It was seen in the Sand Dunes South part of this project that the amplitude response (being dependent on thickness and the change in physical properties) should be a good indicator of the presence of thick, porous Avalon Sand. As such, it is considered that there is a good physical reason for the three attributes used above to be indicators of Avalon thickness. Although the attributes are not independent, each measures the amplitude response in a slightly different way, and the combination of the three is powerful in this case. It should be noted that while the trend from the Sand Dunes seismic model suggested *increasing* amplitude with increasing thickness, the reverse is true at the NDP. There, a roughly inverse relationship between the amplitude measures and porosity zone thickness is observed. This unexpected discrepancy is likely to be the result of the NDP seismic data having higher frequency

content than used in the seismic modeling. As such, the thicker parts of the Avalon Sand at the NDP are *above* the tuning thickness and thus an increase in thickness will result in a decrease in amplitude.

Using amplitude attributes as a basis, a map of the predicted thickness of the Avalon Sand porous interval at the NDP was generated. Anomalously thick areas are indicated for the periphery of the survey area, suggesting that the decrease in signal-to-noise ratio in these areas (due to lower stacking fold and/or reduced migration aperture) is probably affecting the attributes here and giving erroneous values. More or less distinct regions of greater and lesser thickness are indicated in the main body of the seismic data. Two poorly defined N-S trending thick zones (>35 ft of porosity) are present in Section 14, with another in the northeastern part of Section 7. Additionally, there are some E-W trending thick zones, such as along the lower part of Sections 12 and 18. Predicted thicknesses of the porosity zone in the Avalon Sand are generally in the range of 10 to 20 ft. Detailed inspection suggests that the greater thickness are associated with localized flexures, although not all areas with tightly spaced contours are associated with thickening of the Avalon porosity zone. Why these trends do not define clear channels, such as at Sand Dunes South Field, is not readily apparent. It may be that the porosity in the Avalon Sand is related both to depositional and to some other process such as diagenesis. Alternatively, the log-based map from Sand Dunes South may be smoothing over small-scale heterogeneity that is being picked up by the seismic data.

Geologic correlation of the logs in this area does not suggest the presence of channel bodies in the Avalon Sand such as at the Sand Dunes South Field, but rather the presence of a sand "blanket" of variable thickness. However, the two areas are similar in that it appears that subtle structural features present near the top of the Bone Spring had an influence on the preserved thickness of porous sands. It may be that structure-related fracturing and fracture-related diagenesis control where the Avalon Sand will have the best porosity development. In this case, fractures in the Sand Dunes South area might be aligned with the N-S step, whereas both N-S and E-W trending structures are associated with fracturing at the NDP. Petrographic analyses of sidewall cores from the Avalon Sand at the two fields would be useful to help pursue this question further.

Although the porous zone thickness map suggests that some thick porous Avalon Sand is present, the question remains as to whether in fact there is potential production from this sand at the NDP. No production has yet been established from this interval in this area. Sidewall core data have maximum measured porosity and permeability of about 12% and 0.6 md, respectively. Hydrocarbons are present in the sandstones, but the porosity and permeability numbers are slightly low compared to values present where the Avalon is productive (porosity > 15% and permeability > 1 md; e.g., Reference 14). Assuming that there is a relationship between thickness of the porous interval and reservoir quality (e.g., Sand Dunes South), it may be that better reservoir quality will be present at the NDP in the areas where the Avalon is predicted to be thickest.

The structural configuration of the Bone Spring formation at the NDP and the stratigraphic and seismic character of the Avalon Sand at the NDP and the Sand Dunes South Fields were examined. The two main findings are:

1) Movement along basement features is thought to be the main factor affecting the current structural configuration of the Bone Spring formation. This movement is thought to have decreased throughout the deposition of the Bone Spring, but influenced deposition of the Avalon Sand and so may have influenced deposition of the basal Brushy Canyon formation as well.

2) The Avalon Sand can be detected seismically, and the thickness of the porous section can be determined from seismic attributes. This unit is productive where channelized (e.g., at Sand Dunes South) but has not yet been found to be productive at the NDP, where the sand is more sheet-like. It may be that depositional processes, influenced by syn-sedimentary structural development, exert a primary control on reservoir quality. In this case, the Avalon interval may not be prospective in the NDP area or, if it is, the thicker parts of the Member should make the best reservoir.

Further work will concentrate on: a) depth converting the time structure maps using (if possible) the lateral velocity changes implied by the migration velocities, and b) examining the stratigraphic character of the Bone Spring Members in greater detail.

3-D Seismic Interpretation of Cherry Canyon System

Data was analyzed that explains the 3-D seismic interpretation of the Cherry Canyon system. The horizon at about 560 ms in each vertical section is the reference stratal surface from which the Cherry Canyon interpretation was done (**Fig. 5**). This surface is associated with a robust reflection peak that extends over the total 3-D image area, and it should be reasonably conformable to stratal surfaces with the Cherry Canyon. Two surfaces are found at 26 ms and 56ms, respectively, below the reference surface at 560 ms. Both surfaces are conformable to the reference. These two horizons bracket the Cherry Canyon reservoir facies that was positioned in the 3-D seismic image space by the VSP time-vs-depth control from NDP Well #25. The horizon that is midway between the 26 ms an 56 ms surfaces passes through the Cherry Canyon position at NDP Well #24 (which was defined to be at a depth of 4200 ft) and is conformable to the Bone Spring horizon almost 400 ms deeper in the image space (the Bone Spring is below 1.0 sec: and is not shown in any of these vertical sections). This midpoint horizon was not used in the Cherry Canyon interpretation. It was shown to emphasize the fact that seismic stratal surfaces more than 3000 ft apart vertically and on opposite sides of the Cherry Canyon system (one above and one below) are reasonably conformable. The conclusion was that a narrow data window that brackets the Cherry Canyon system could be constructed by using either the Bone Spring horizon (at about 1000 ms) or the horizon at about 560 ms as a reference stratal surface. The better choice of the two reference horizons is the one that is closer to the Cherry Canyon target, which would be the horizon at 560 ms. All Cherry Canyon interpretation was done using data window boundaries that were conformable to this 560 ms horizon.

The position of the Cherry Canyon reservoir facies in the 3-D seismic image at NDP Well #24 is critical for determining which reflection peak or trough is associated with the thinbed unit. The waveform characteristic that is genetically related with the Cherry Canyon facies position at a depth of 4200 ft is the reflection peak that is midway between the 26 ms and 56 ms below the reference surface.

Cherry Canyon reservoirs are seismic thin-bed units as are the Brushy Canyon "K" and "L" reservoirs that have been interpreted previously. Using the guidelines established in the Brushy Canyon work (and in other seismic thin-bed studies), the amount of net pay in the Cherry Canyon section should increase as the amplitude of the associated reflection peak increases. Consequently, the seismic attributes that should indicate Cherry Canyon drill sites would be those that react to this seismic reflection peak amplitude within the data window bounded by the 26 ms and 56 ms horizons.

Appropriate amplitude-sensitive attributes that should indicate Cherry Canyon net pay were considered: maximum peak amplitude, average peak amplitude, average absolute amplitude and average reflection strength. These attributes show that the amplitude peak associated with the Cherry Canyon facies at NDP Well #24 increases in elliptical areas that trend southwest-northwest and are located west and north of NDP Well #24. Equally robust amplitude behaviors occur in a large area spanning NDP Wells #1, 5, 6, 10, 20, and 29. However, this latter area of increased amplitude responses creates a false indication of Cherry Canyon net pay and is associated with a different depositional sequence than the sequence that creates the Cherry Canyon facies at NDP Well #24 and west and northwest of NDP Well #24.

Two sequences were identified, sequence A being the one that is genetically related to the attractive Cherry Canyon facies in NDP Well #24, and sequence B being the one genetically related to the less attractive Cherry Canyon facies, found in the eastern wells. There is no way to tell from the seismic data alone which sequence has the more attractive net pay possibilities. However, once well control defines which depositional sequence is preferred, then the 3-D seismic data can be used to map the areal amplitude behavior in the targeted sequence.

Seismic Conclusions

Several conclusions can be drawn from this portion of the seismic work.

- Deep, Morrow-related faults appear to have a genetic relationship to the bench-step model that is being used to describe Brushy Canyon deposition.
- The top of the Bone Spring Carbonate reflects the deep structure and provides the depositional surface for the Basal Brushy Canyon interval.
- The bench-step sequence is carried through to the shallow Cherry Canyon interval in the upper Delaware.
- A north-south bench running through Sections 12 and 13 and a step running north-south through Sections 11 and 14 is evident at each stratigraphic level.

Reservoir Compartments and Boundaries

Further work was done in the Brushy Canyon "L" zone to compare the correlation of the boundaries between the observed data, the seismic interpretation and the geostatistics/seismic

attribute analysis. A strong correlation is seen between production and testing analysis, seismic interpretation, and the geostatistics/seismic attribute analysis. These data were refined to predict drainage areas and depositional trends.

Drainage Areas

To estimate drainage areas for each well, decline curves were extrapolated to predict the ultimate oil recovery from each well, and this value was divided by the oil recovery per acre. This resulted in a calculated drainage area, presented in **Table 1**. The calculated drainage area was then adjusted depending on the seismic amplitude in the "L" zone.

The seismic amplitude coincides with areas that are compartmentalized or continuous. Negative amplitudes of 0 to -20 are associated with areas that are compartmentalized, and areas with negative amplitudes from -20 to -60 are in areas where the zones are more continuous. Analysis of the areas that are compartmentalized indicates that approximately 75% of the pay interval is continuous enough to contribute to production. The drainage areas associated with these wells are multiplied by a factor of 1.33 to adjust for zones that are not continuous and this yields an indicated drainage area.

By comparing the indicated drainage area to the drainage area that the well was predicted to drain, based on governmental proration units or stimulation designs, a drainage ratio "D" can be calculated. If the wells are effectively draining the area they are designed to drain, the drainage ratio should be 1.0. Presented in **Table 1**, the drainage ratios range from 0.15 to 1.23, with 53% ranging from 0.75 to 1.25.

The other factor influencing oil recovery is interference from offset wells and the resulting depletion. Depletion is evidenced by initial gas-oil-ratios (GORs) that are above 2,000 SCFG/BO as shown in **Fig. 6.** The initial wells and wells drilled away from developed areas had initial GORs of less than 2,000, and wells drilled in developed areas or later in the development of the field had GORs of 2,000-14,000 to 1.

This results in the early wells, such as #1, #11 and #13, recovering more oil than predicted and later wells such as NDP Wells #12, #29 and #38 recovering less oil than predicted. The drainage areas for each of the areas predicted in the production interference analysis are shown in **Table 2.**

A strong correlation was found between the transmissivity (kh/μ), the number of sacks of sand used in the frac treatment, and the ultimate recovery. The ultimate recovery can be approximated by the following relationship:

$$BO = ((kh/\mu) \times \text{No. Sx. Sand})^{.5} \times 1{,}000$$

A closer correlation is obtained by adding the drainage ratio to the equation to obtain:

$$BO = ((kh/\mu) \times \text{No. Sx. Sand})^{.5} \times \text{Drainage Ratio} \times 1{,}000$$

The results of this correlation can be seen in **Fig. 7.** This correlation will be explored further to determine the applicability to forecast recoveries from Delaware wells, and as a tool to size fracture treatments.

Reservoir Compartments

The analysis of reservoir, seismic, and production data has led to an interpretation of the major reservoir compartments in the "L" Zone. Using a reservoir simulator model to match GOR history and to estimate the reservoir pressure, bottomhole pressure (BHP) history was developed for each well. These data are presented in **Table 3.**

The BHP data were then used in a nearest-neighbor analysis to determine areas of the reservoir with common pressure characteristics (see **Fig. 8**). The nearest neighbor analysis coupled with the cumulative production vs. rate analysis and the geostatistical analysis (described later in this report) have provided an interpretation of the major reservoir compartments in the "L" Zone.

The current interpretation indicates a series of well defined compartments that are identified by production interference, seismic data, and pressure history. These compartments are shown in **Fig. 9** and are summarized in **Table 4.**

There is good correlation of the boundaries between the observed data and the seismic interpretation. Boundaries are interpreted to exist where there is a large contrast in amplitudes, from a high negative amplitude area to a low negative amplitude area. This interpretation is supported by the analysis[2] of instantaneous frequencies prepared earlier by Dr. Bob Hardage. His interpretation indicated compartments that were more complex than this interpretation, but may be more accurate in the light of reduced recovery efficiency of wells in areas he described as "highly compartmentalized." This may indicate that some individual sands are continuous from well to well and some sands are very limited in their areal extent.

This work will continue for the purpose of aiding in the prediction of drilling locations with minimal pressure depletion and compartments that have not been drained. NDP Well #36 will test this theory when a directional/horizontal well is drilled into the seismic anomaly north of NDP Well #15. This pod may be a separate compartment that is defined by a large contrast in seismic amplitudes surrounding this anomaly.

Geostatistics and Reservoir Mapping

The second annual report[2] discussed the results of the L-zone amplitude-porosity correlation used to locate NDP Well #29. Because the porosity encountered in Well #29 was 40% less than that predicted from correlation, two different approaches were investigated to forecast spatial reservoir properties. A production interference analysis was conducted to define flow units, and several mapping techniques were used to describe the static reservoir properties.

Well Interference and Flow Units

Oil rate versus cumulative production curves were reviewed for evidence of interference resulting from the production from newly completed off-set producing wells. Conventionally, the information is graphed as Cartesian plots; however, changes in the slopes of the curves are more readily observed with a semilog presentation, as seen in **Fig. 10.**

The early- and late-time slopes, along with the initial GOR, are given in **Table 5.** The wells are tabulated in chronological order of completion.

There is no established slope for NDP Wells # 29 and #38, due to insufficient production history. The wells were assigned to the flow units based on the a slope change and the initial GOR. A high initial GOR with a constant slope indicates that pressure depletion had occurred at the time of completion. In this case flow units are defined as areas exempt from interference from off-set wells. The flow units are illustrated in **Fig. 11.**

Statistical Analysis of Flow Units

Several mapping techniques were used to describe the spatial distribution of the L-zone static reservoir properties. Since the objective is to optimize the placement of drilling locations, the hydrocarbon pore volume ($h*\phi*S_o$) was the reservoir mapping parameter. The $h*\phi*S_o$ parameter was developed from log information and was mapped with a conventional, nearest neighbor ($1/r^2$) technique, with a kriging technique based on a spherical variogram model, and with a fractal model. As displayed in **Fig. 12**, the maps resulting from the three different methods are similar. The fractal map (**Fig. 12d.**) includes only the wells shown in **Fig. 11.**

In addition to the static reservoir properties mapped in **Fig. 12**, a "drill here" map requires an estimate of bottomhole pressure to be complete. Estimates of the distribution of dynamic reservoir properties such as pressure are best obtained by matching the past reservoir history with a simulator which was reported in the second annual report.[2] However, a pressure indicator is included in the map shown in **Fig. 13.** Bottomhole pressure was estimated based on the current producing GOR data and PVT data. These estimates were normalized with the 2950 psi discovery pressure and then used to calculate $h*\phi*s_o*p/p_i$. These values were used to generate the fractal map in **Fig. 14.**

The delineation of the flow units (**Fig. 11**) coupled with the hydrocarbon pore volume/BHP map (**Fig. 14**) suggests that future primary development should be towards the northwest under the playa lakes.

Geostatistics and Interwell Properties

Targeted infill drilling is a development option at the NDP. In an effort to better define interwell properties and to understand the reservoir northwest of the current producing wells, two geostatistical analyses were conducted. The first focused on extrapolating with the variogram

developed from well data to an area northwest of NDP Well #13. The second was a scoping study applying ordinary kriging to slices from the 3-D seismic survey to estimate the density of 2-D lines required to capture the features apparent in the 3-D grid. The study provides insight to the number of 2-D lines required to characterize the reservoir under the playa lake.

Geostatistical Extrapolation

Interwell reservoir properties were estimated with three different mapping techniques: a conventional nearest neighbor ($1/r^2$) method, a kriging method, and a fractal algorithm. The net thickness, porosity, and oil saturation arithmetic average values for the K-zone and the L-zone were determined by well log analysis. The interpolated porosity values between the wells are shown in **Fig. 15** for the three different mapping methods. The left column illustrates the K-zone values and the right column presents the L-zone values. The basic pattern provided by the three mapping methods is similar for the L-zone while the K-zone is less similar.

Previous work in the project[2] suggests that the area under the playa lakes to the northwest be considered for further primary development. Geostatisical mapping algorithms were used to estimate reservoir properties between NDP Well #13 and an imaginary well drilled 7500 ft northwest of that well. The imaginary well expands the **Fig. 15** study area to the northwest. The average net thickness, porosity, and saturations of the NDP wells and the non-Unit wells to the southeast of the NDP were included in the analysis. For the purposes of this analysis, the software variogram range in the expanded study area was a constant 5280 ft for the parameters investigated. Variogram data points and spherical models of thickness, porosity, oil saturation, and hydrocarbon pore volume (HCPV) are presented in **Fig. 16.**

A range of imaginary well properties (half and twice the average for the NDP) are shown in **Table 6**. The average, half-average, and twice-average properties were used to generate kriged maps, which include the imaginary well. The saturation values are the average for the entire zone which result in the low values for oil saturations for both zones.

The variogram range for the imaginary well was constant at 5280 ft. Gray-scale kriged maps of the hydrocarbon pore volume are presented in **Fig. 17. Figure 17** is arranged in two columns for both the K-zone and the L-zone. The half-average value at the imaginary well is shown in the top sets of figures, the average value is the middle set, and twice the average value is the bottom set of maps.

The distribution of the properties is readily evident in color maps, however the gray-scale maps are best viewed remembering that the average value given in **Table 6** is the value of the imaginary well located in the northwest corner of the maps in the middle of the page. The maximum L-zone values are northeast of NDP Well #13. The L-zone minimum HCPV values are to the south and southeast of the study area.

NDP Wells #5, 6, 14, 20, and 29 are perforated in the L-zone only. NDP Well #25 is perforated in the K-zone only. Only the open zones were included in the composite HCPV versus Estimated

Cumulative Oil plot shown in **Fig. 18.** If the correlation coefficient was better than 16%, **Fig. 17** could be used to in conjunction with **Fig. 18** as a method to select vertical well drilling *locations* with some confidence. The unknown effect of free gas saturation (pressure) on estimating oil saturation could be a cause of the poor correlation coefficient.

The 16% correlation coefficient provides little help in selecting future vertical well locations based on HCPV maps. However, **Fig. 19** maybe useful. The x-axis is the HCPV and the y-axis is the probability of drilling a vertical well with an estimated ultimate recovery of 75,000 bbl. Probability is determined by selecting the wells to the right of 75,000 bbl in **Fig. 18**. The HCPV values were arranged in descending order, and the cumulative number of the wells was divided by 16 (total number of wells in **Fig. 18**) to arrive at a value for the y-axis. **Figure 19** confirms that the greater the HCPV value, the greater the chance of drilling a 75,000 bbl well. If the price of oil is greater than $18/bbl, a 75,000 bbl well will pay out.

Returning to **Fig. 17**, this analysis suggests that the properties at the imaginary well 7500 ft northwest of NDP Well #13 do not influence the properties within 1500 ft of the well when the variogram range is 5280 ft. Multivariate analytical tools, described later in this report, were investigated as a means of correlating 3-D seismic attributes with the same well properties as used in this geostatistical study.

2-D Seismic Analysis

The purpose of this geostatistical research is to gain insight into the density of 2-D seismic lines required to identify reservoir features that are present in the 3-D data set. An experimental 2-D data set was constructed from the NDP K-zone 3-D survey. The 3-D attribute map shown in **Fig. 20a** shows the spatial distribution of the average reflective strength across the K-zone. This map serves as a reference for identifying reservoir features that result from combining increasing numbers of 2-D slices. A geostatistical algorithm, ordinary kriging, was used to merge the one-dimensional 2-D lines into a two-dimensional presentation.

Landmark's SuperSeisWorks, software was used to cut the 2-D slices from the 3-D survey. The Landmark documentation states that in sandstone reservoirs the average reflective strength is thought to be related to spatial changes in lithology or is evidence of channels. Gviz, a geostatistical mapping program was used to integrate the 2-D lines.

A reference map, **Fig. 20a**, covers about four sections with a bin spacing of 55 ft. The gray scale bar correlates with a spatial variation in the attribute of 10-80 units.

The kriging algorithm upscales the bin spacing of 2-D slices to 255 ft which results in the smooth features in the kriged maps as opposed to the fine detail seen in the reference map. The remaining maps in **Fig. 20** consist of slices bisecting the 3-D dataset: two slices (**Fig. 20b**), four slices (**Fig. 20c**), and five slices, including a diagonal (**Fig. 20d**).

The density of the 2-D slices is increased in **Fig. 21**, which repeats the reference map. **Fig. 21b** includes a fifth, non-diagonal slice. Note that the east half, dark features seen in the reference map

are now evident. The six equally-spaced 2-D lines in **Fig. 21c** capture many of the original features. All of the major features in the reference map are captured with the kriged map using 10 equally-spaced 2-D slices, as illustrated in **Fig. 21d**.

Thus, in this example, a network of 2-D lines spaced about 1050 ft apart were used to generate kriged maps that capture the major features seen in the 3-D data set with 55 ft bin resolution. The example visually demonstrates the potential to identify reservoir features with multiple 2-D datasets.

Seismic Attribute Analysis

In the prior section, the potential value of geostatistical techniques for estimating interwell reservoir properties, with infill drilling as a possible goal, was discussed. However, NDP wells primarily cover the center part of the available seismic survey, so a methodology was tested for relating reservoir properties at the wellbore to sets of seismic attributes in order to extrapolate reservoir properties beyond the area directly constrained by wells and to predict reservoir properties across the whole field. Seismic attributes have recently been the focus of renewed interest for evaluating reservoir properties. Well data gives very precise information on the reservoir properties at specific field locations with a high degree of vertical resolution, while 3-D seismic surveys can cover large areas of the field, yet reservoir properties are not directly observable, in part due to relatively poor vertical resolution.

A new technique was developed that utilizes a nonlinear multivariable regression to correlate statistically selected seismic attributes to reservoir properties (ϕ, S_w, and net pay). The new technique uses seismic attributes as inputs with porosity, water saturation, and net pay as outputs. The regression equations allow a prediction of these three reservoir properties in areas without direct well control. When mathematical relationships between the attributes and wellbore parameters from wireline logs are established, maps of reservoir properties were computed for the location of each seismic bin (every 110 ft) across the NDP for the "K" and "L" intervals.

Data

The two primary sources of data required for this method are well data and seismic attribute data. The well data used in this study are tabulated in **Table 7**. Over 80 seismic attributes were extracted from the NDP seismic data volume for the two horizons using the PostStack and Pal tools of the Landmark Graphics seismic interpretation suite. Extracted attributes were averaged across the entire interval of both the "K" and "L" horizons, respectively, and the well data from each of the 19 wells used in the study were also averaged across the respective intervals. Thus the output maps presented later in this report represent interval-averaged values for the respective reservoir properties.

Attribute Selection

It is computationally infeasible to use all of the extracted attributes in individual nonlinear regressions for reservoir properties, therefore a fuzzy-ranking algorithm[16] was used to select attributes best suited for predicting individual reservoir properties. The algorithm statistically

determines how well a particular input (seismic attribute) could resolve a particular output (reservoir property at the wellbore) with respect to any number of other inputs. Each attribute is assigned a rank, which allows a direct estimation of which attributes would contribute the most to a particular regression.

The fuzzy ranking algorithm was applied to select the optimal inputs (attributes) for six output cases: "K" porosity, "K" net pay, "K" water saturation, "L" porosity, "L" net pay, and "L" water saturation.

Multivariable Nonlinear Regression

Linear regression for reservoir properties was not feasible for this study, as the relationships between input and outputs were poorly defined by individual attributes. We elected to use a nonlinear regression using the fast-converging, feed-forward, back-propagation conjugate gradient algorithm (neural network) implemented in-house at the PRRC. Two neural network architectures were used in the study, both of which were minimized in order to maintain a satisfactory ratio of training data to weights (coefficients of the regression equation). The two networks are graphically illustrated below.

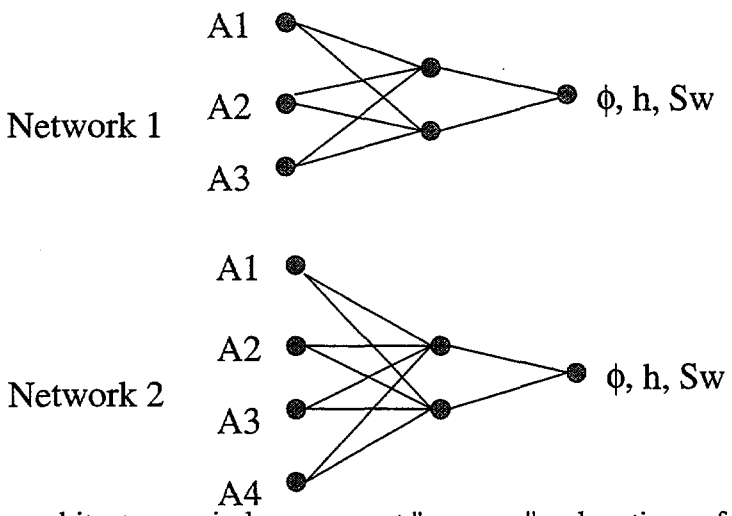

In these architectures, circles represent "neurons" or locations of nonlinear functions, while each line represents a coefficient applied to these equations. A back-propagation feed-forward algorithm, such as the conjugate gradient algorithm that was used, is "trained" using known inputs and outputs. For this study, reservoir properties are known at the locations of the wellbore intersections with the interval of interest. Seismic attribute data from the same seismic bin that contains the well is correlated to wellbore values of porosity, net pay, or water saturation in an iterative process using the neural network. **Table 8** shows which attributes and network were used in regressions for each reservoir property in the two intervals of interest.

Training and Testing

It is customary to test the robustness of a solution by holding some data out for testing. Since only 19 control points were available, the networks were trained using all 19 points, and then tested by removing sets of three wells, retraining the network with 16 control points, and then using that network to predict the three withheld points. This exercise was applied three times for each property and interval, withholding differing sets of three points for each test. **Figure 22** shows the results of training with all 19 points, and three test sets for the "L" interval porosity regression. It is evident that the network has resolved porosity in a robust fashion, and that the tool may be used to predict porosity in other areas of the field. **Figure 23** shows the 19 point networks for the other reservoir properties of the "L" and the "K" intervals. These regressions were also tested in the same manner, and had similar results.

Predicting Fieldwide Reservoir Properties

The regression relationships (architecture and weights) were used to compute maps of fieldwide porosity, net pay, and water saturation, which were displayed in Landmark's SuperSeisworks Map view. Screen images of these properties, and computed phi*h and h*phi*S_o maps are presented in **Figs. 24 to 28**. In general these maps fit expectations based on other geostatistical techniques and reservoir understanding.

Maps of Reservoir Properties

For each of the maps sets in **Figs. 24 to 28**, the same color bar was used, though ranges may vary slightly. Therefore these maps highlight relative differences between the "K" and "L" intervals.

Figure 24 shows "K" and "L" interval porosity maps predicted using the regression relationships. Both "K" and "L" horizons show patterns of distinct, or isolated porosity, and the "L" porosity map compares favorably with compartment maps produced independently. **Figure 25** shows "K" and "L" interval net pay maps. The "K" horizon shows much more variation in pay than the "L" zone, which is reasonable considering that the "K" interval is discontinuous and may pinch out, while the "L" interval is considered to be reasonably continuous across the study area. Lineations in the NW corner of the "L" net pay map may indicate facies changes, or onlap deposition and subsequent compartmentalization. **Figure 26** shows "K" and "L" interval water saturation maps. In general the "K" interval appears to very water wet, except in distinct pods, which may represent possible drilling targets. The "L" interval is wet, in a more uniform fashion, though an area of high water saturation in the NW corner, which is up-dip, may be due to compartmentalization as indicated in **Fig. 25**.

Figures 27 and 28 show phi*h and h*phi*S_o maps for the "K" and "L" horizons. The phi*h maps in **Fig. 27** are useful as an indicator of where sufficient porosity-thickness exists within the field. The "K" horizon shows a good deal of variability, with relatively lower phi*h in areas where the "K" zone is interpreted to pinch out. The "L" interval phi*h illustrated in **Fig. 27b** shows a more uniform distribution of pay porosity, though some thinner and thicker areas do exist. Fine detail

across the middle portion of the map may assist in determining compartmentalization of porosity, as net pay is relatively uniform across that region. The hydrocarbon pore volume maps in **Figs. 28a and 28b** for the "K" and "L" intervals, respectively, include information on oil saturation (1-Sw) and essentially illustrates where the oil is located in the field. The water wet "K" interval shows only isolated pods of good production potential, while the less wet "L" interval shows strong undrilled potential production in the SE quadrant of Section 11, the SW and NW quadrants of Section 7, and the west half of Section 14. Areas to avoid drilling for the "L" interval might include the east half of Sections 7 and 18, the SW quadrant of Section 13, and the SE quadrant of Section 14.

Reservoir Simulation Forecasts

Reservoir simulation forecasts focused on evaluating carbon dioxide injection in the proposed pilot area and the evaluation of the Apprentice/Merlin reservoir simulator from Gemini Solutions, Inc. to evaluate a planned horizontal well.

Modeling a Horizontal Well

Apprentice is a graphical preprocessor that can be used to construct engineering representations of geology for several reservoir simulators. In addition to Merlin, it supports VIP® (Landmark) and Simbest™ (Scientific Software-Intercomp). Merlin is a black oil-like simulator designed for use with PCs.

The target for this software evaluation is NDP #36, the planned horizontal well to be located in Blocks 11 and 12 (see **Fig. 29**). This well will terminate in a horizontal segment approximately 1120 ft long. It is anticipated that four vertical fractures will be induced hydraulically to promote drainage around the horizontal segment of the well. The purpose of the simulation is to determine:

- whether the Apprentice/Merlin simulator can handle horizontal wells with fractures
- what the initial conditions are in the drainage area of NDP #36
- what recoveries can be expected from the proposed configuration of NDP #36
- whether additional fractures would provide additional cost-benefit

Three models of increasing complexity were developed. Each had four layers corresponding to the L_a, L_b, L_c, and L_d intervals, respectively. They differed in their treatment of the induced fractures. The simplest model treated the four planned fractures as a column of 10-foot gridblocks; the most complex model treated them as a column of one-foot blocks. It was possible to make runs through historical production data with the coarse model, but not the refined models. At the outset of this effort, it was hoped that the Apprentice/Merlin package would allow somewhat faster turn-around than the SGM/Eclipse software used previously by the reservoir simulation team. There does seem to be a steep learning curve with this package, so that this first use of the Apprentice/Merlin did not progress as quickly as had been hoped.

Miscible Recovery Simulations

The Nash Draw miscible recovery evaluation progressed in two areas: evaluation of the NDP core with CT scanning and simulation of the carbon dioxide (CO_2) injection pilot area.

The core provided to the University of Houston was sampled as a 4x1 inch plug. The plug was subjected to CT scanning for a determination of three-dimensional porosity distribution. The data were analyzed to present several displays of porosity distribution from the complete three-dimensional data as well as simple x-y plots of the distribution. The data were used in a simulated miscible displacement study to determine the connected porosity and a quantitative measure of bypassing to be expected. These data were then utilized in the simulation to limit the amount of recovery by miscible injection.

Prior work on the NDP pilot area produced simulations with a qualitative match of history to March, 1997. These results and data were used as the basis of simulations of miscible injection in the pilot area. Although a different reservoir simulator was required for the miscible injection study, the history match for the miscible cases was qualitatively the same as that previously obtained even though lower hydrocarbon gas density was used in the miscible gas study. History match for gas production from the five wells in the pilot area (NDP Wells #1, 5, 6, 10, and 14) show typical solution gas drive performance with initial high GORs decreasing as the reservoir is depleted. Since the pilot location for this study is no longer under consideration for the field trial, further history matching was not performed, since it is likely only minor differences in results would follow. Instead, several predictions of miscible and immiscible injection were performed to obtain qualitative results for these different recovery mechanisms.

Several prediction simulations were performed with CO_2 for both miscible and immiscible injection scenarios. For the miscible injection cases, simplifying assumptions were made because no laboratory data were available. In particular, the miscible injectant was assumed to have properties of pure carbon dioxide and to be first-contact miscible with the reservoir oil. To compare the different prediction cases, oil production was calibrated by adjusting the flowing bottomhole pressure at the beginning of the prediction cases so that the oil production rate was similar to the field-observed rates. With the constant bottomhole pressure as a boundary condition, predictions were then made from the end of history for 11 years to March 1, 2008. Injection was assumed to begin immediately after the end of the history match, although in reality a delay of at least 2 years would be required for project implementation. Injection was based on 120 MSCF/D of gas injectant - either miscible or immiscible. This volume was based on the volume of immicible gas required to maintain pressure in the reservoir. A water-alternating-gas (WAG) scenario was also simulated. In this case the injection bottomhole pressure was limited to 5000 psi with a WAG ratio of about 4:1 water to carbon dioxide.

Simulations compared a base case of continued operations with no injection to a total of 9 prediction cases for various recovery scenarios: (1) convert NDP # 1 to injector - 120 MSCF/D CO_2 miscible, (2) convert NDP # 5 to injector - 120 MSCF/D CO_2 miscible, (3) convert NDP # 6 to injector - 120 MSCF/D CO_2 miscible, (4) convert NDP # 10 to injector - 120 MSCF/D CO_2 miscible,

(5) convert NDP # 14 to injector - 120 MSCF/D CO_2 miscible, (6) infill injector - 120 MSCF/D CO_2 miscible, (7) infill injector - 4:1 WAG, (8) infill injector - 60 MSCF/D CO_2 miscible, and (9) infill injector - 120 MSCF/D immiscible injection. The infill injector was located at the center of the pilot area between wells NDP # 1, 6, 10, and 14.

Simulation results for miscible injection in the NDP pilot area indicate that carbon dioxide injection may well be a viable alternative for improved oil recovery for this field. For the eight different CO_2 miscible scenarios, increased oil recovery was observed compared to a continued operations case (see **Table 9**). Increased oil recoveries ranged from a low of 40 MSTB to a high of 110 MSTB or an increase in recovery of from 2-5% of OOIP. In contrast, immiscible hydrocarbon gas injection showed little increase in oil recovery.[2] These results coupled with a reasonable recovery per MCF of CO_2 injected indicate that further investigations should be made into CO_2 miscible injection.

To continue work on a new pilot area several steps need to be taken. Several assumptions which were made in the initial miscible simulations need to be validated. In particular, even if first-contact miscibility does not occur, swelling of the oil from immiscible CO_2 injection may also result in significant oil recoveries. Reservoir fluid behavior tests should be performed, especially with carbon dioxide as one of the components. Better characterization of the reservoir in the vicinity of the new pilot area should be obtained to assess the practicality of initiating an injection test. Based on these preliminary results, CO_2 breakthrough should occur in less than one year even in the most optimistic situation. This indicates that a well-designed and simulated pilot could provide timely information for use in a full-field implementation.

These forecasts indicate that areas of the NDP already under production may be candidates for miscible CO_2 injection, if pressures have not declined too much. If implemented before the pressure has declined below about 1500 psi, CO_2 injection might be successful, but economics would need to be assessed. Although miscible CO_2 flooding appears to be a viable method at the NDP, a low-cost source of the gas is not currently available in the vicinity of the NDP.

Technology Transfer

Transferring technical information generated during the course of this project is a prime objective of the project. Toward this objective, Strata has participated in several meetings and workshops to promote the dissemination of information. A summary of technology transfer activities during the third year of the project is outlined below.

SPE Paper 38916 - A paper titled "Reservoir Characterization as a Risk Reduction Tool at the Nash Draw Pool," was presented at the SPE Annual Technical Conference and Exhibition in San Antonio, Texas in October, 1997. This paper was also presented at the 1998 Permian Basin Oil and Gas Recovery Conference in Midland, Texas on March 23-26, 1998. The paper SPE has received favorable reviews from the SPE Editorial Review Committee; it will be revised and considered for publication in SPE Reservoir Evaluation & Engineering.

SPE Paper 38868 - A paper entitled "Implementation of a Virtual Enterprise for Reservoir Management Applications," which describes the Nash Draw virtual team, was presented at the SPE Annual Technical Conference and Exhibition in San Antonio, Texas in October, 1997.

Logging Workshop - The log analysis techniques used at the Nash Draw Project were presented at a workshop entitled "Advanced Applications of Wireline Logging for Improved Oil Recovery Workshop." The workshop was organized by BDM Oklahoma and the PTTC and was held at the CEED in Odessa, Texas on November 13, 1997.

SPE Paper 39775- A paper entitled "Using Reservoir Characterization Results at the Nash Draw Pool to Improve Completion Design and Stimulation Treatments." was presented at the 1998 Permian Basin Oil and Gas Recovery Conference in Midland, Texas on March 23-26, 1998.

Core Workshop - Nash Draw core and associated material was exhibited at a core workshop held in Midland, Texas on February 26, 1998. The workshop was sponsored by the Permian Basin Section/SEPM for cores from DOE projects in the Permian Basin.

Project Review - In June 1998, several members of the Nash Draw team met with NPTO personnel in Tulsa, OK to discuss results obtained in Phase I of the NDP project and to present proposed plans for Phase II. A Project Evaluation Report has been prepared that provides details of the Phase I results as well as recommendations for the continuing the project in Phase II.

Liaison Meeting- Strata has provided information concerning the NDP to individual operators on a one-on-one basis. An example of this was a presentation made in June 1998 to Altura Energy in Houston, Texas. Altura was interested in the reservoir characterization and 3-D seismic activities at the NDP.

Phase I Project Report: A final report of Phase I activities was prepared along with this Third Annual Report.

Internet Homepage: The new address of the Website for the Nash Draw project is: http://baervan.nmt.edu/REACT/Links/nash/strata.html. This site includes an interactive map of logs and production data for the project and the most recent annual (second annual) report including graphics.

PRRC personnel presented results of the research from the NDP project involving the correlation of 3-D seismic attributes with well properties and capturing 3-D seismic images from 2-D seismic lines. These presentations were made in Dallas, Ft. Worth, Midland, and Odessa, Texas to more than 80 individuals in 14 companies representing major oil companies and independent producers. Comments from the various company meetings indicate that interest in 3-D seismic attribute analysis is universal to both majors and independents.

CONCLUSIONS

Several conclusions can be drawn from the work done during the third year of the NDP project.

The faults and depositional character of the deeper structures (Morrow and Bone Spring) provide the depositional surface for the shallower sequences and creates the bench-step surface being used to describe the Brushy Canyon reservoir.

The Brushy Canyon reservoir is much more complex than originally interpreted. Many sands are compartmentalized and are not always continuous from well to well which affect flow paths between wells.

Drainage of primary reserves can occur over large areas with little reduction in recovery efficiency.

Miscible CO_2 flooding appears to be viable in areas of the NDP if reservoir pressure has not declined too much; however, a low-cost source of the gas is not available in the vicinity of the field. A more viable option would be pressure maintenance with injection of lean hydrocarbon gas.

Maximization of recovery will be a combination of targeted drilling, selective completions, and pressure maintenance designed to drain reservoir compartments.

A Fuzzy Ranking algorithm was used to help decide which seismic attributes are most useful for evaluating reservoir properties.

Multivariable nonlinear regression (Neural Networks) were used at the NDP project to correlate well and seismic data with the goal of predicting interwell reservoir properties and extrapolating to regions beyond well control.

REFERENCES

1. Murphy M.B., et al: "Advanced Oil Recovery Technologies for Improved Recovery from Slope Basin Clastic Reservoirs, Nash Draw Brushy Canyon Pool, Eddy County, New Mexico," Report, Cooperative Agreement DE-FC-95BC14941, submitted to the U.S. Department of Energy (October 1996).

2. Murphy M.B., et al: "Advanced Oil Recovery Technologies for Improved Recovery from Slope Basin Clastic Reservoirs, Nash Draw Brushy Canyon Pool, Eddy County, New Mexico," Second Annual Report, Cooperative Agreement DE-FC-95BC14941, submitted to the U.S. Department of Energy (October 1997).

3. Murphy M.B., et al: "Advanced Oil Recovery Technologies for Improved Recovery from Slope Basin Clastic Reservoirs, Nash Draw Brushy Canyon Pool, Eddy County, New Mexico," Third Annual Report, Cooperative Agreement DE-FC-95BC14941, submitted to

the U.S. Department of Energy (October 1998).

4. Martin F.D., et al: "Advanced Reservoir Characterization for Improved Oil Recovery in a New Mexico Delaware Basin Project," *Proc.* Fourth International Reservoir Characterization Technical Conference, Houston, (1997) March 2–4, 703-26.

5. Martin, F.D., et al: "Reservoir Characterization as a Risk Reduction Tool at the Nash Draw Pool," paper SPE 38916 presented at the 1997 SPE Annual Technical Conference & Exhibition, San Antonio, Oct. 5-8, *Proc.* Reservoir Engineering, 751-66.

6. Stubbs, B.A., et al: "Using Reservoir Characterization Results at the Nash Draw Pool to Improve Completion Design and Stimulation Treatments," paper SPE 39775 presented at the 1998 SPE Permian Basin Oil and Gas Recovery Conference, Midland, March 23-26.

7. Martin, F.D., et al: "Implementation of a Virtual Enterprise for Reservoir Management Applications," paper SPE 38868 presented at the 1997 SPE Annual Technical Conference & Exhibition, San Antonio, Oct. 5-8.

8. Hardage, B.A., et al: "3-D Seismic Imaging and Interpretation of Brushy Canyon Slope and Basin Thin-Bed Reservoirs, Northwest Basin," *GEOPHYSICS,* Vol. 63, No. 5 (September-October 1998) 1507-1519.

9. Hardage, B.A., et al: "Using 3-D Volumes of Instantaneous Frequency to Interpret Reservoir Compartment Boundaries Across an Area of Complex Turbidite Deposits," *GEOPHYSICS*, Vol. 63, No. 5 (September-October 1998) 1520-1531.

10. Hart, B.S.: "3-D Seismic: What Makes Interpreters Tick?" *The Leading Edge*, 16, 1114-1119 (1997).

11. Gawloski, T.F.: "Nature, Distribution, and Petroleum Potential of Bone Spring Detrital Sediments Along the Northwest Shelf of the Delaware Basin," in The Leonardian Facies in W. Texas and S.E. New Mexico and Guidebook to the Glass Mountains, Cromwell, D. and Mazzullo, L.J. (eds.), SEPM, Permian Basin Section Publication No. 87-27, 85-105 (1987).

12. Handford, C.R., and Loucks, R.G.: "Carbonate Depositional Sequences and Systems Tracts - Responses of Carbonate Platforms to Relative Sea-level Changes," in Carbonate Sequence Stratigraphy: Recent Developments and Applications, R.G. Loucks and J.F. Sarg (eds.), AAPG Memoir 57, 3-41 (1993).

13. Hart, B.S.: "New Targets in the Bone Spring Formation, Permian Basin," *OGJ*, v. 95, No. 30, 85-88 (1997).

14. Montgomery, S.L.: "Permian Bone Spring Formation: Sandstone Play in the Delaware Basin, Part II - Basin," *American Association of Petroleum Geologists Bulletin*, v. 81, 1423-1434 (1997).

15. Marfurt, K.J., Scheet, R.M., Sharp, J.A., and Harper, M.G.: "Suppression of the Acquisition Footprint for Seismic Sequence Attribute Mapping," *Geophysics*, v. 63, 1024-1035 (1998).

16. Lin, Y., and G. A. Cunningham: "A New Approach to Fuzzy-Neural System Modeling," *IEEE Transactions on Fuzzy Systems*, 3 No. 2, 190-198 (1995).

Table 1. Drainage Areas.

WELL #	1-1-98 ULTIMATE RECOVERY BBLS.	RECOVERY BO/ACRE	CALCULATED DRAINAGE AREA ACRES	SEISMIC CONTINUITY INDEX	INDICATED DRAINAGE ACRES	DESIGNED DRAINAGE ACRES	"D" DRAINAGE RATIO	"P" TOTAL TRANSMISSIVITY (OIL AND WATER)	"S" SAND SX.	P-S-D INDEX	INITIAL GOR SCFG/BO
1	61,776	2,758	22.40	1.33	29.90	40	0.7475	11.620	357	48,146	2,000
5	71,722	2,926	24.51	1.33	32.72	40	0.8180	12.826	410	59,322	1,200
6	57,525	2,627	21.90	1.33	29.23	40	0.7308	13.772	410	54,914	1,400
9	58,822	1,545	38.07	1.33	50.82	60	0.8471	4.687	1,150	62,189	1,600
10	48,162	1,613	29.86	1.33	39.86	40	0.9965	6.374	358	47,601	1,800
11	142,173	2,896	49.09	1.00	49.09	40	1.2273	14.050	410	93,151	1,200
12	34,580	2,957	11.69	1.00	11.69	60	0.1949	14.699	1,900	24,429	14,000
13	87,644	5,325	16.46	1.33	21.97	40	0.5493	22.460	540	60,493	1,500
14	89,832	3,085	29.12	1.33	38.87	40	0.9718	15.235	479	83,016	2,600
15	124,598	2,964	42.04	1.00	42.04	60	0.7006	20.890	1,860	138,104	2,700
19	134,171	2,205	60.85	1.00	60.85	60	1.0141	9.380	1,192	107,217	1,500
20	55,240	1,937	28.52	1.33	38.07	40	0.9518	7.721	410	53,549	5,900
23	41,315	1,710	24.16	1.17	28.15	60	0.4691	4.338	2,239	46,232	5,700
24	128,583	3,338	38.52	1.33	51.42	60	0.8570	10.746	1,894	122,276	2,500
25	9,721	1,178	8.25	1.33	11.02	60	0.1836	0.975	1,650	7,364	4,700
29	23,335	2,640	8.84	1.00	8.84	60	0.1473	19.609	2,169	22,785	8,100
38	27,504	1,389	19.81	1.00	19.81	60	0.3301	10.477	1,798	33,982	6,200
TOTAL	1,196,703		474.09		564.35	860.00				1,064,773	

Table 2. Unit Areas.

Unit	Wells	Area, ac.
A	1, 6, 9, 10, 14, 20, 23 & 25	265.92
B	11, 12 & 13	82.75
C	5, 29, & 38	61.37
D	24	51.42
E	15	42.05
F	19	60.85
	Total	564.36

Table 3. Bottomhole Pressure vs. Gas-Oil Ratio.

WELL #	GOR 1993	BHP PSI	GOR 1994	BHP PSI	GOR 1995	BHP PSI	GOR 1996	BHP PSI	GOR 1997	BHP PSI	GOR 1998	BHP pSI
1	2.85	2100	8.54	1100	10.95	800	9.56	150	8.35	100	4.37	50
5	1.28	2800	6.38	1250	8.81	950	6.29	1275	8.47	950	9.01	900
6	1.45	2800	6.10	1280	7.64	1050	6.61	1225	6.66	1250	8.57	950
9	1.68	2800	3.01	1950	3.82	1750	12.06	400	11.60	300	8.59	200
10	0.77	2900	4.72	1550	7.23	1100	6.90	1200	13.52	500	14.06	400
11	0.96	2900	1.40	2700	4.82	1525	4.08	1800	5.26	1400	4.81	1500
12									13.03	800	15.98	500
13	1.07	2900	1.94	2400	4.96	1500	5.71	1400	6.16	1300	8.40	960
14	1.05	2900	5.79	1470	7.91	1050	12.69	400	10.81	300	9.34	200
15			1.92	2400	3.91	1725	5.74	1400	10.20	800	13.39	600
19			1.54	2600	6.87	1200	8.23	1000	5.94	1330	6.31	1250
20			2.96	2000	6.09	1300	3.80	1525	6.21	1300	7.59	1100
23					5.10	1480	7.10	1120	18.56	500	20.77	400
24					1.71	2500	3.85	1750	4.64	1550	4.26	1620
25							3.75	1760	4.45	1600	7.17	1125
29									7.00	1150	9.38	860
38									3.71	1750	5.59	1400

Table 4. Compartmentalization Interpretation.

Wells in Common Compartments	Comments
1, 6, 9, 10, 12, 14, 19, 20, 23, 25, 29 & 38	This area exhibits communication between wells, and later wells such as #12, 29, & 38 exhibited partial pressure depletion and high initial GORs.
5	This well does not exhibit major communication with neighboring wells.
11 & 13	These wells do not exhibit major communication with neighboring wells.
15	May have minor communication with #23, which would indicate a trend through #15, 23, 29, & 38.
24	This well does not exhibit communication with neighboring wells.

Table 5. Production Interference Analysis.

Well	Flow Unit	Early Slope	Late Slope	Initial GOR, mcf/bbl
9	A	1.8	2.4	1.6
1	A	3.5	6.7	2.0
10	A	3.0	4.8	1.8
13	B	1.3	3.2	1.5
6	A	1.7	3.7	1.4
11	B	1.8	constant	1.2
14	A	2.5	constant	2.6
5	C	3.6	constant	1.2
20	A	3.3	constant	5.9
15	E	1.5	constant	2.7
19	F	1.4	constant	1.5
24	D	1.4	constant	2.5
23	A	3.9	constant	5.7
12	B	7.3	constant	14.0
25	A	1.4	constant	4.7
29	C			8.1
38	C			6.2

Table 6. Average Properties of the Study Area.

	K-zone	L-Zone
Thickness, ft	50.3	33.8
Porosity, %	9.9	11.3
Oil Saturation, %	12.4	22.0
Phi-h, %-ft	484.5	366.0
HCPV, fraction	0.593	1.436

Table 7. Well and Seismic Attribute Analysis.
Well Data for K and L intervals

Well	"K" Net Pay	"K" Porosity	"K" Sw	"L" Net Pay	"L" Porosity	"L" Sw
U-1	40.5	5.9	80.8	35.5	10.1	41.7
U-5	65.0	8.7	87.3	31.0	10.5	59.1
U-6	44.5	11.1	87.9	25.0	13.4	41.4
U-9	63.5	8.7	88.7	31.5	7.2	76.1
U-10	47.0	10.2	91.1	14.5	12.5	43.2
U-11	37.0	10.9	81.3	28.0	12.8	37.9
U-12	59.5	9.1	90.9	46.5	11.3	53.6
U-13	52.5	12.3	70.1	38.5	13.6	40.6
U-14	45.0	11.5	72.9	26.5	13.1	42.5
U-15	39.0	10.8	93.3	28.0	13.7	40.3
U-19	67.5	4.2	93.6	19.5	12.4	39.9
U-20	22.5	12.6	84.6	20.5	13.1	47.8
U-23	34.5	10.5	79.0	6.5	13.0	38.8
U-24	52.5	11.8	75.1	23.0	12.9	47.7
U-25	35.0	11.2	81.5	12.0	9.2	88.5
U-29	52.5	11.7	92.7	31.5	12.1	42.1
U-38	57.0	14.3	96.5	23.5	11.0	97.0
T-FEE-1	56.5	8.5	98.2	43.0	10.7	75.4
T-FED-1	71.0	6.6	99.4	67.0	10.5	75.9

Table 8. Average Interval Attributes Used for the Nonlinear Regressions.

Reservoir Property	Architecture	CC	Attributes
"K" Porosity	Network 1	0.89	Max peak frequency Avg absolute frequency Isochron
"K" Net-Pay	Network 2	0.86	Max peak frequency Avg absolute frequency Avg absolute amplitude Isochron
"K" Water Saturation	Network 1	0.83	Avg reflection strength Avg peak frequency Isochron
"L" Porosity	Network 1	0.88	Isochron Avg instantaneous frequency Energy half-time
"L" Net Pay	Network 1	0.80	Avg max peak amplitude Avg RMS amplitude Avg Peak amplitude
"L" Water Saturation	Network 1	0.84	Avg instantaneous phase Avg trough amplitude Energy half-time

Table 9. Reservoir Simulation Forecasts for CO_2 Injection.
11-Year Recovery Forecasts for NDP Pilot Area

Continued Operation

	Predicted Oil Recovery, MSTB
No CO_2 Injection	267.6

Miscible CO_2 Injection, 120 mscf/D

Injection Well	*Predicted Oil Recovery, MSTB*
1	325.1
5	318.1
6	377.6
10	366.5
14	341.1
Infill	365.1
Infill (4:1 WAG)	311.2
Infill*	320.0
Infill (Immiscible)	280.0

*60 mscf/D

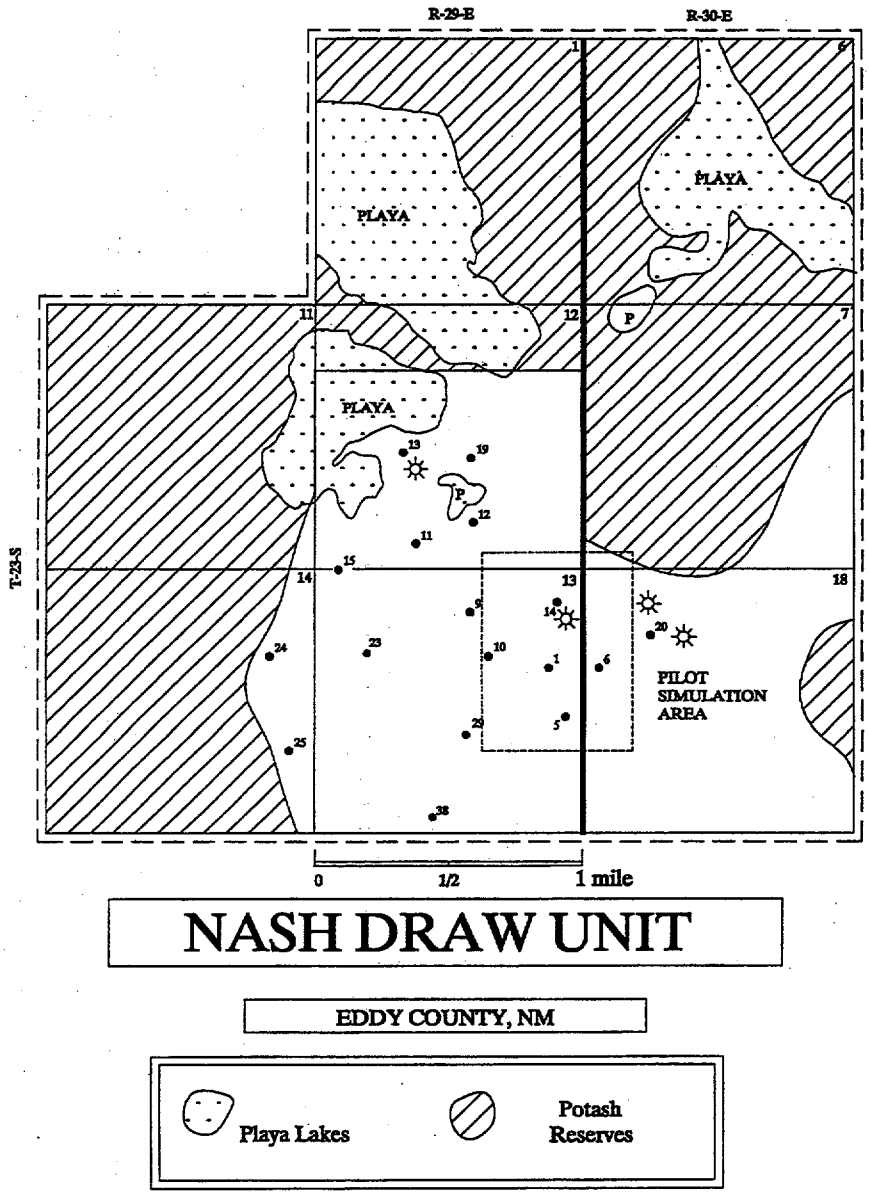

Fig. 1. Map of NDP.

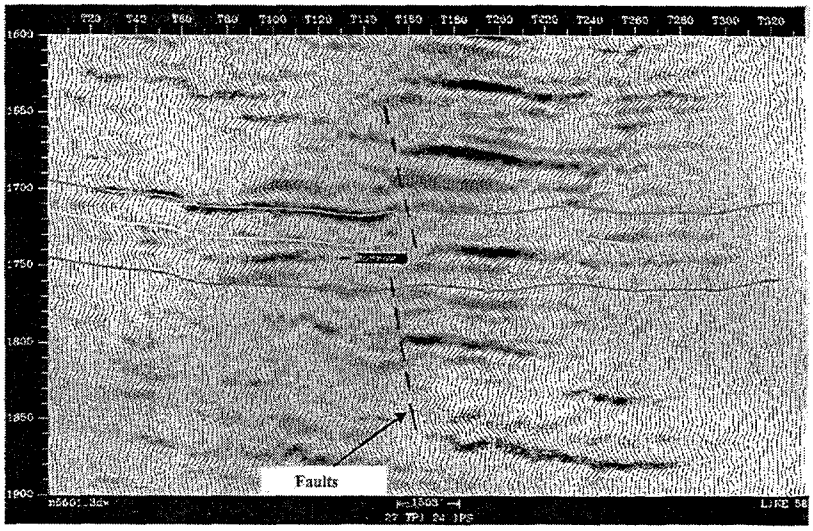

Fig. 2. Morrow level faults.

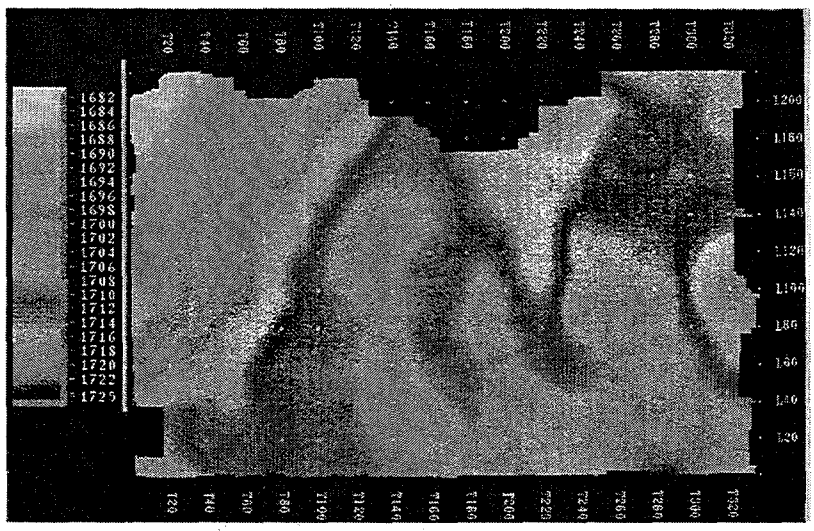

Fig. 3. Morrow time structure map.

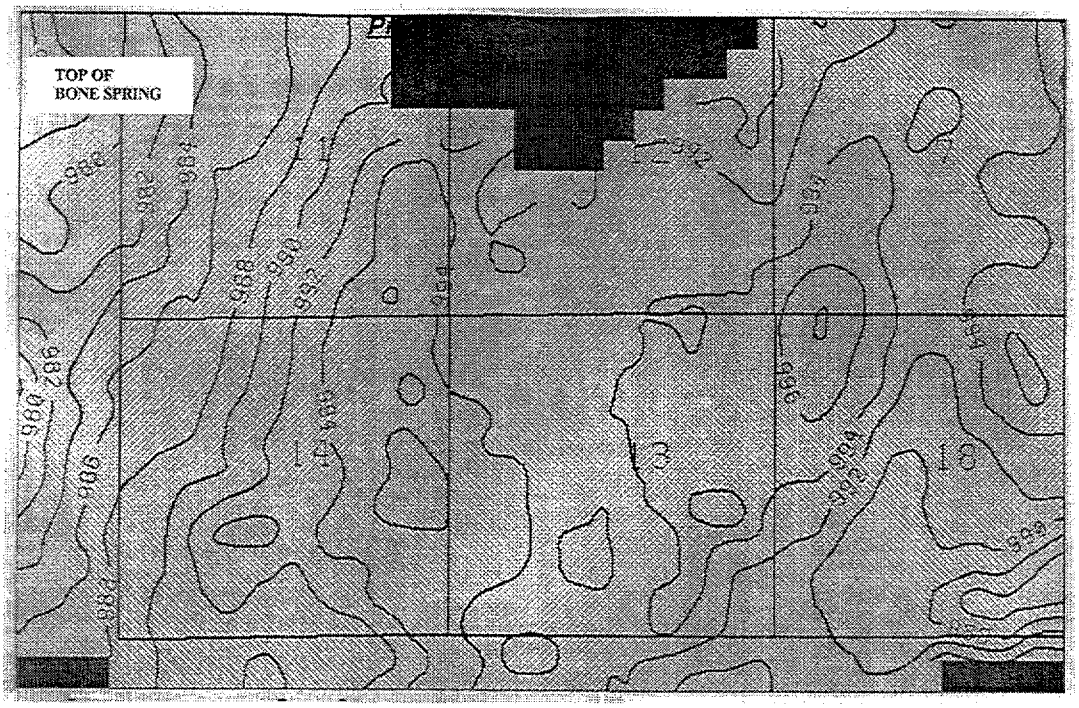

Fig. 4. Bone Springs Amplitude.

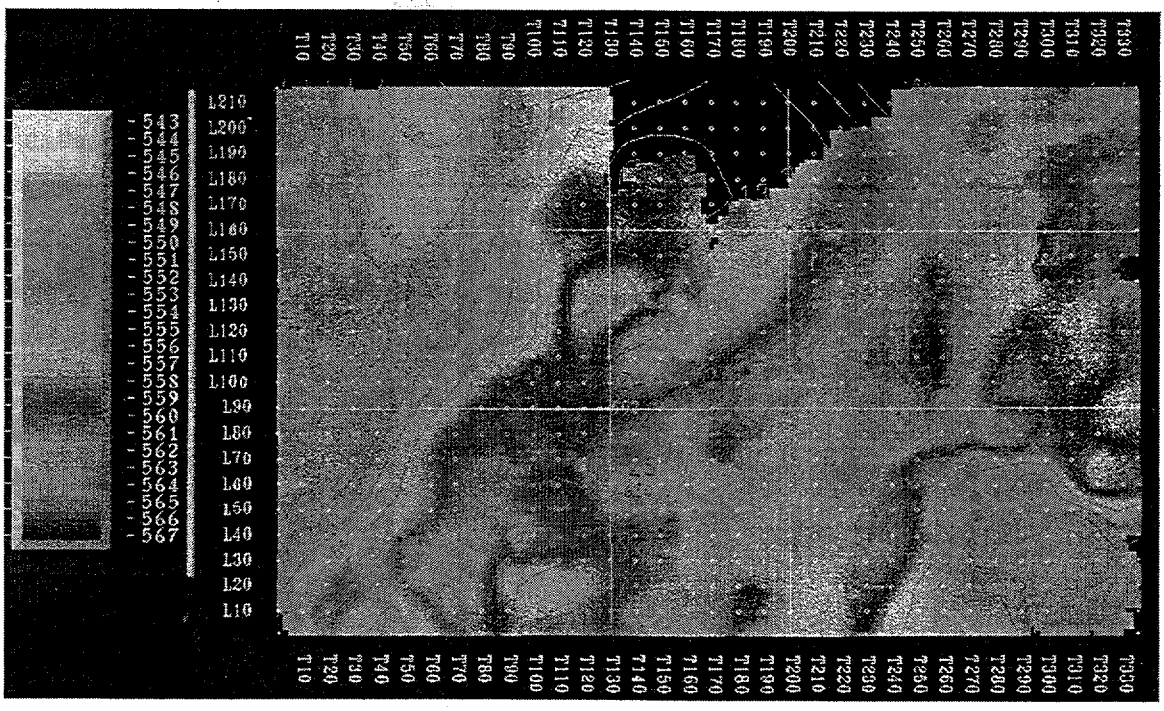

Fig. 5. Cherry Canyon.

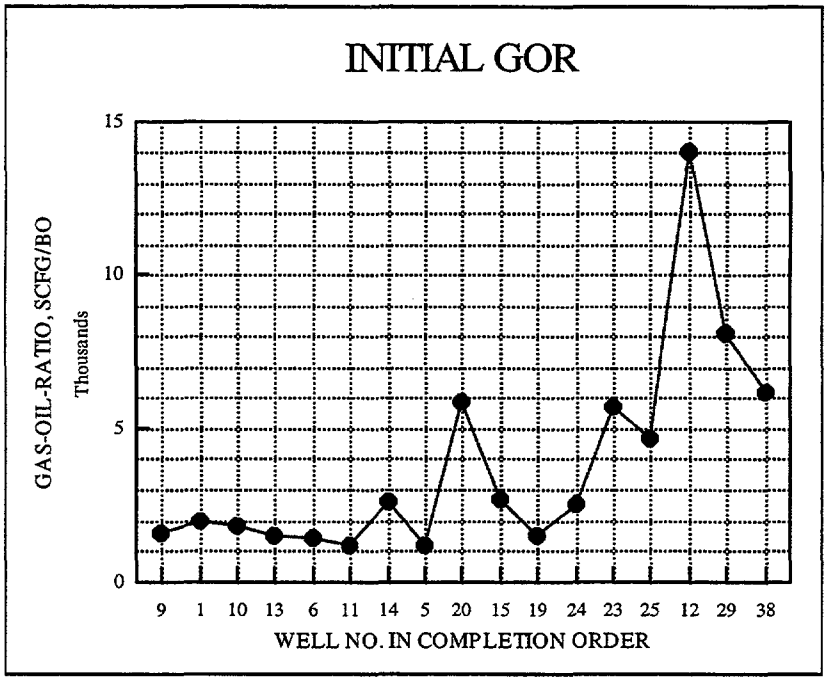

Fig. 6. Initial GOR.

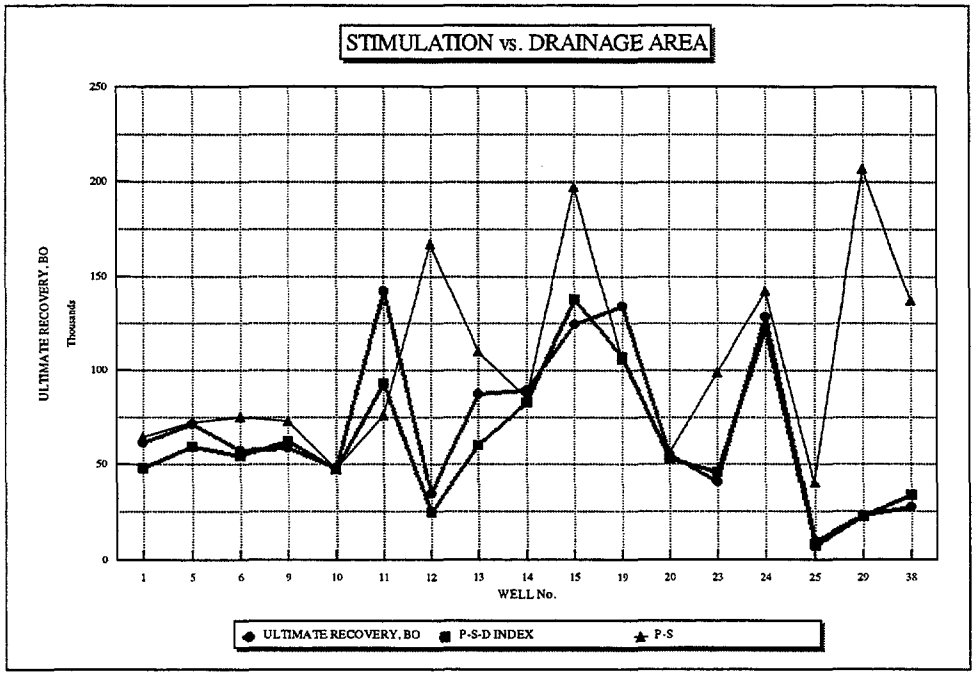

Fig. 7. Ultimate recovery correlation.

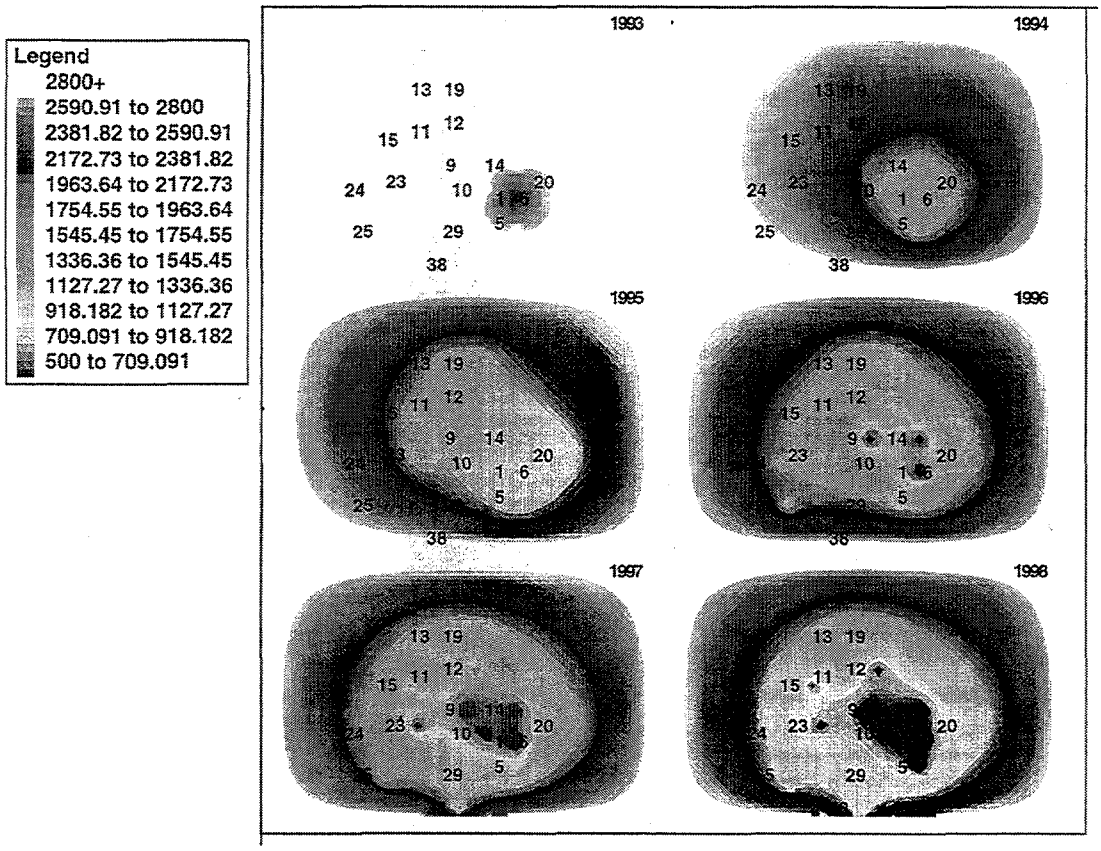

Fig. 8. Nearest neighbor analysis of estimated bottomhole pressure.

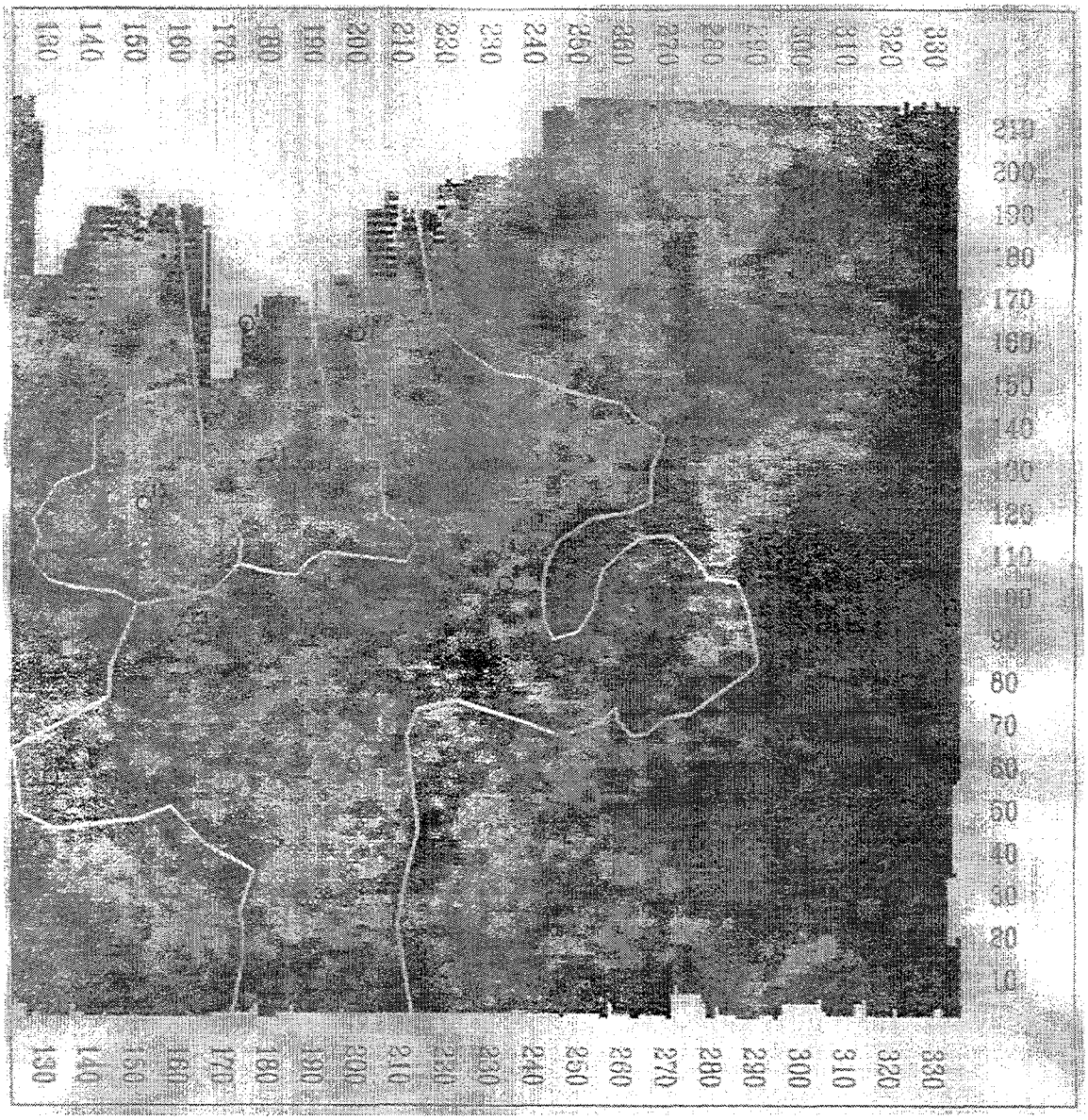

Fig. 9. Interpretation of nearest neighbor, interference and seismic data to determine major reservoir compartments.

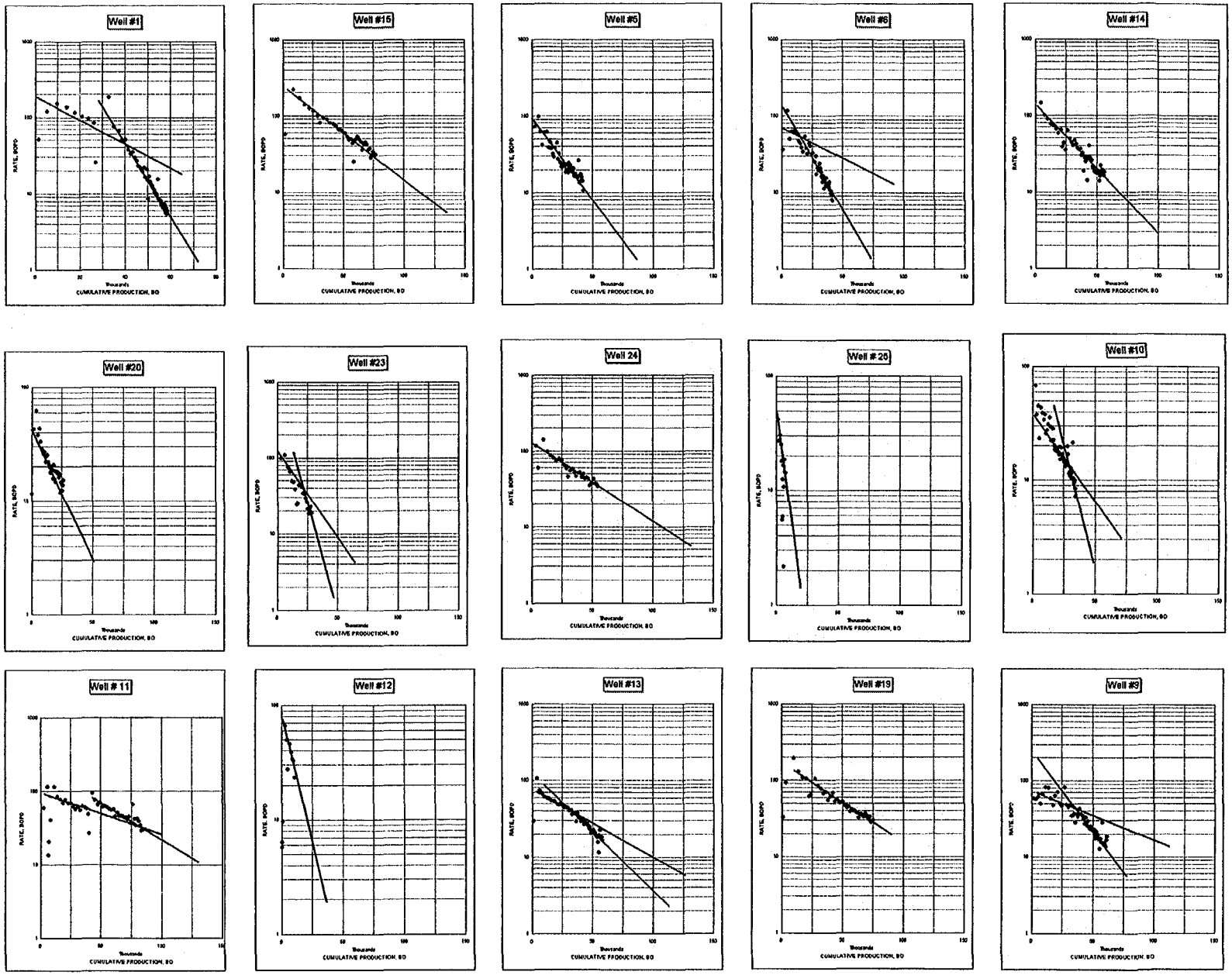

Fig. 10. Cumulative production vs. rate.

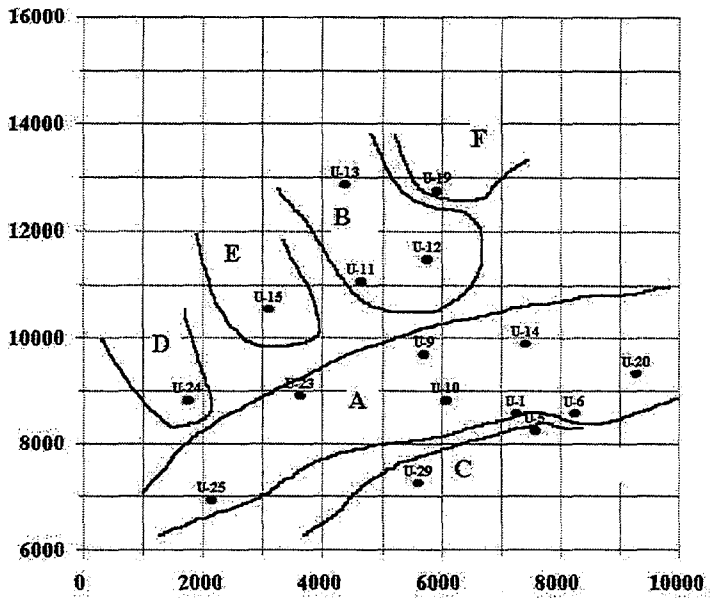

Fig. 11. Flow units (A, B, C, D, E & F) derived from interference analysis.

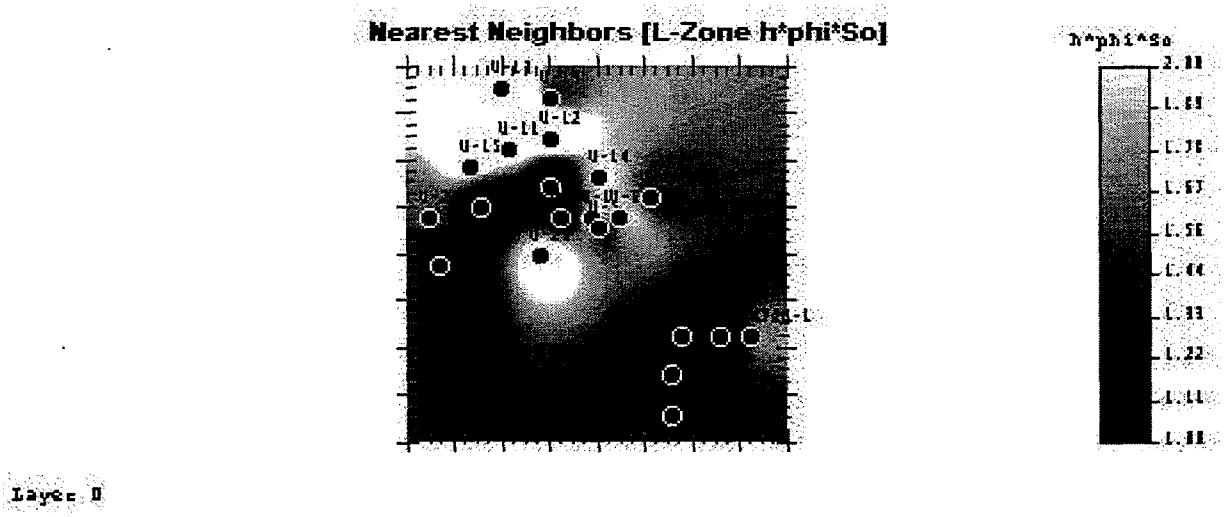

Fig. 12a. Map of hydrocarbon pore volume generated with nearest neighbor techniques.

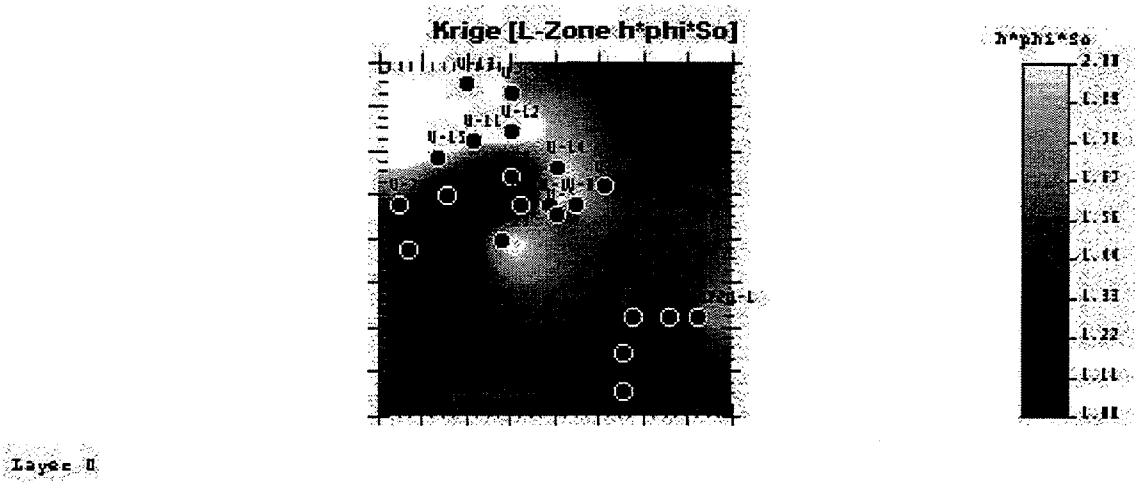

Fig. 12b. Kriged map of hydrocarbon pore volume generated with spherical variogram.

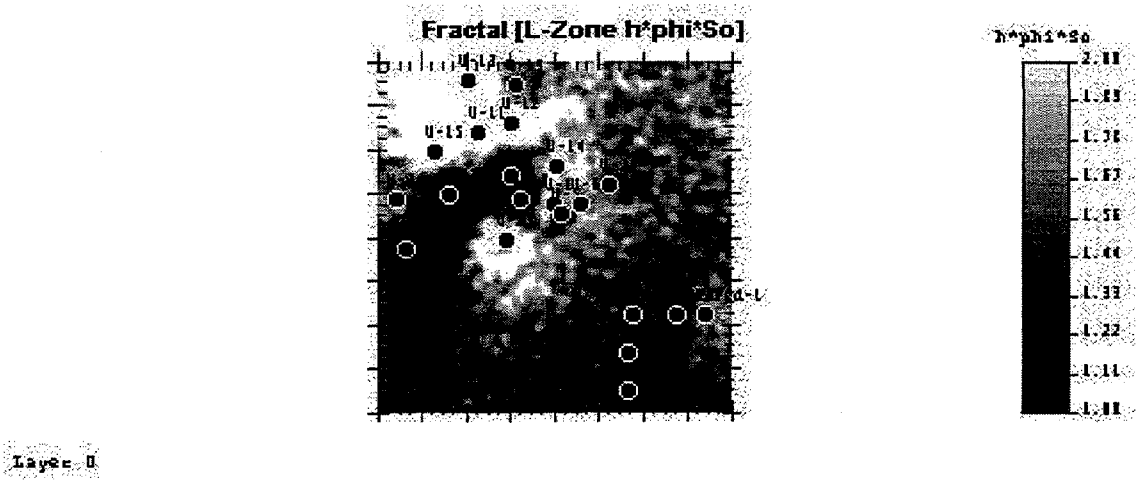

Fig. 12c. Map of hydrocarbon pore volume generated with fractal algorithm

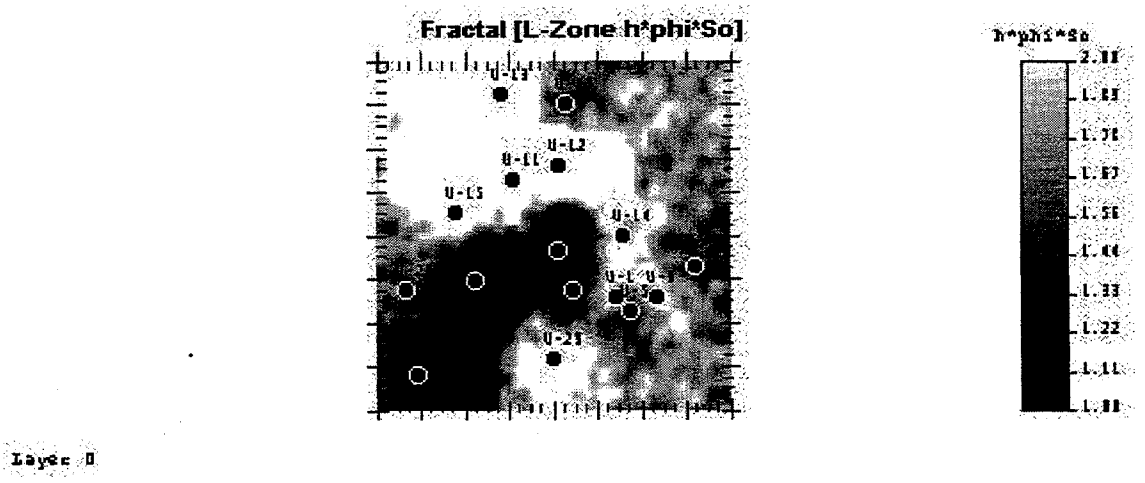

Fig. 12d. Fractal hydrocarbon pore volume map rescaled to include only the unit wells seen in Fig. 2.

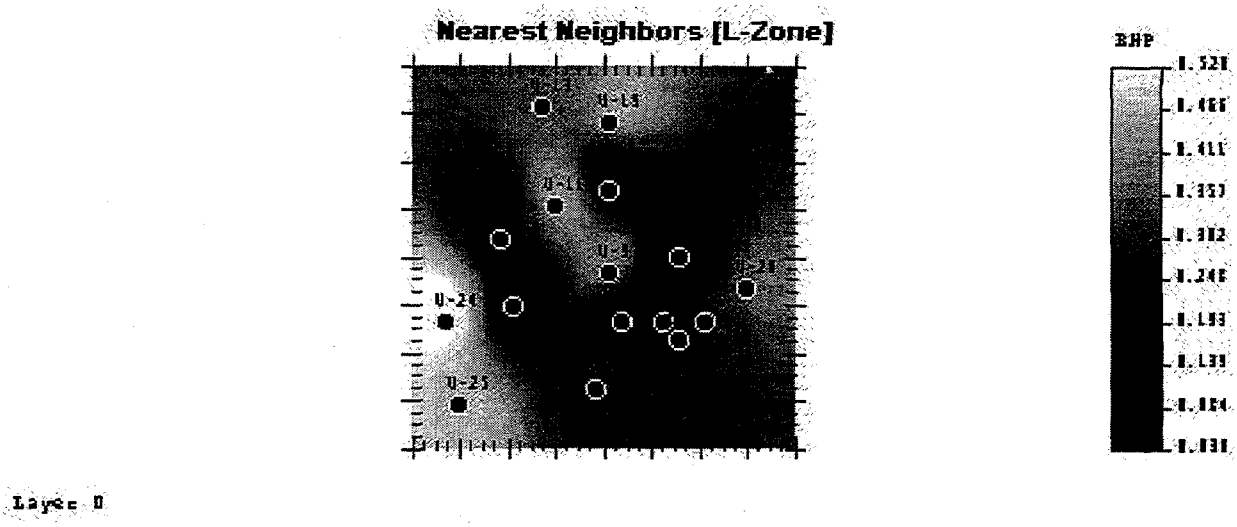

Fig. 13. Bottomhole pressure from conventional method.

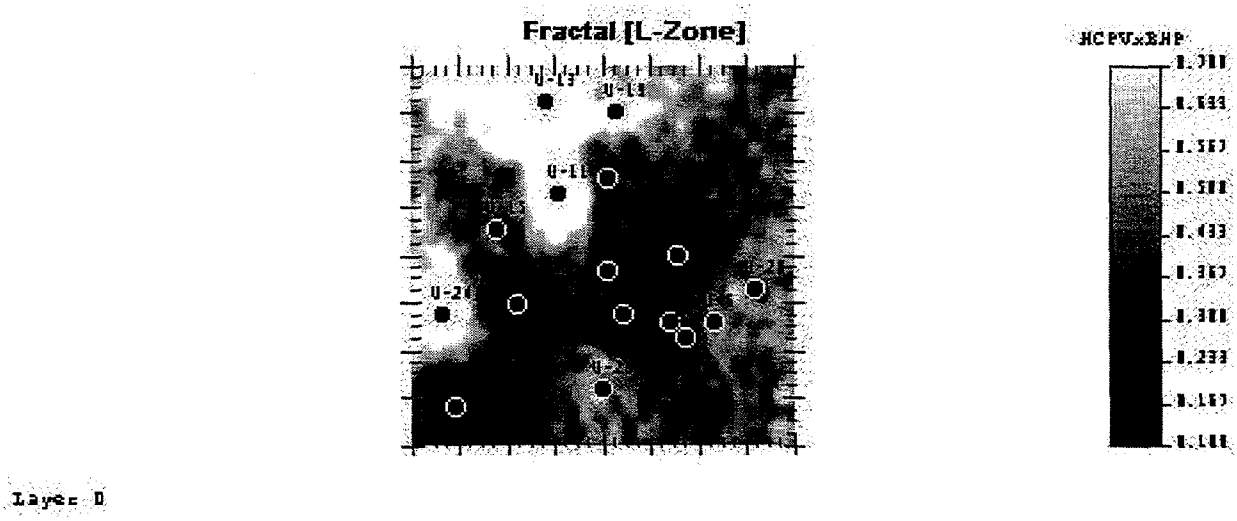

Fig. 14. Fractal hydrocarbon pore volume map conditioned with normalized bottomhole pressure.

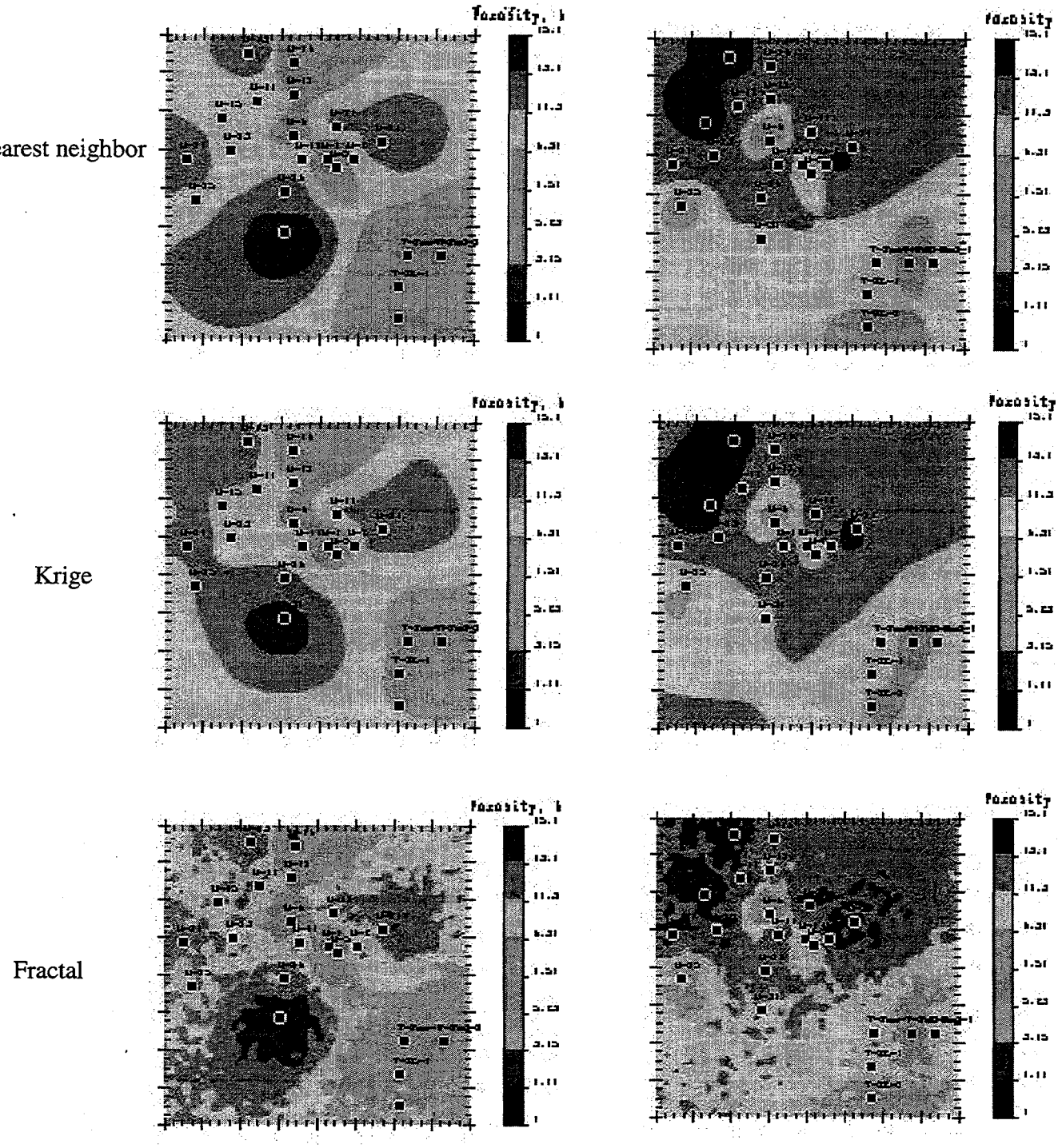

Fig. 15. Porosity distribution estimated by conventional nearest neighbor, ordinary kriging, and fractal mapping techniques.

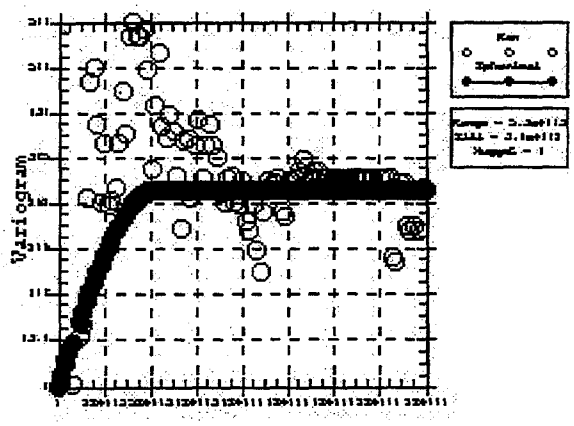

Thickness

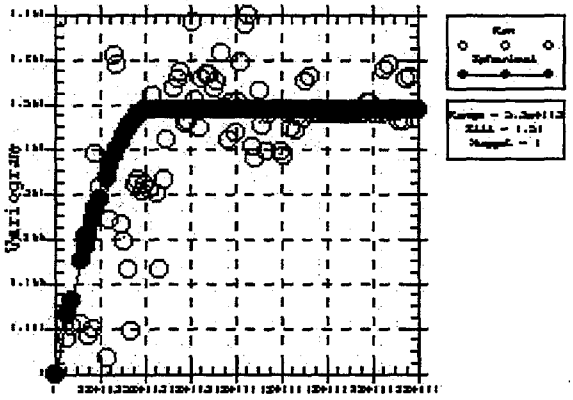

HCPV

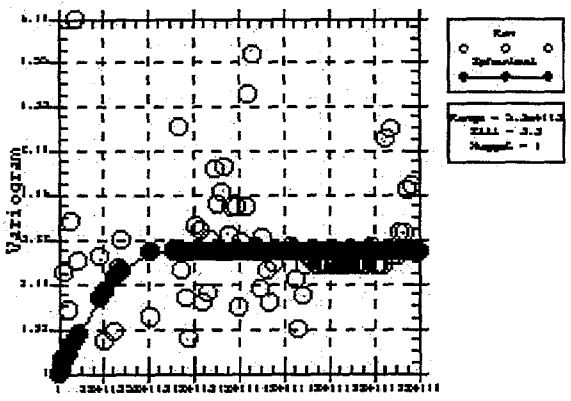

Porosity

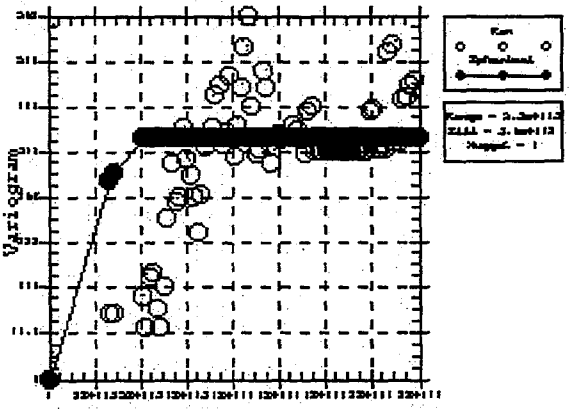

Saturation

Fig. 16. Variograms of thickness, porosity, oil saturation and HCPV spherical models in the L-zone. Constant 5,280 ft range.

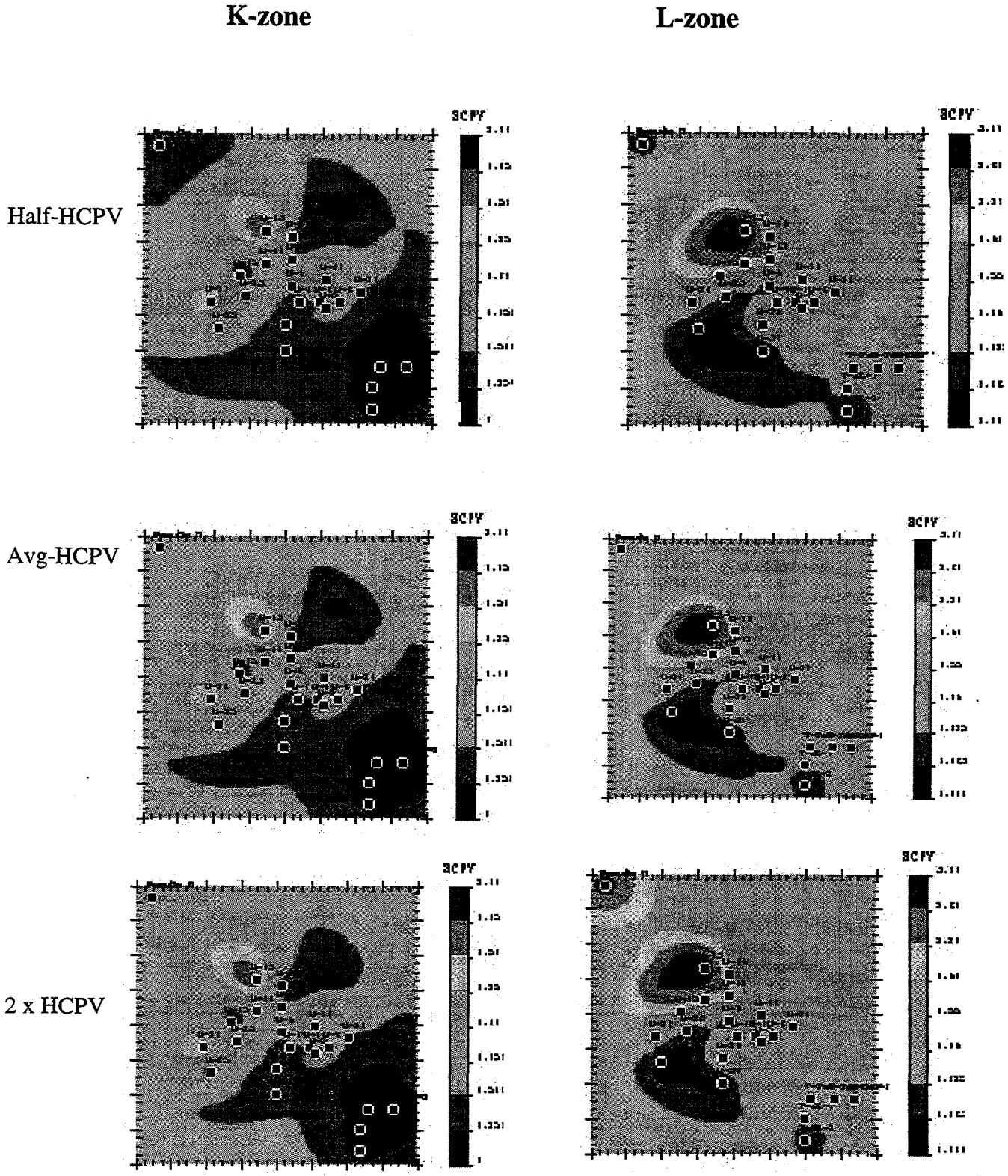

Fig. 17. Estimated K-zone and L-zone HCPV distribution.

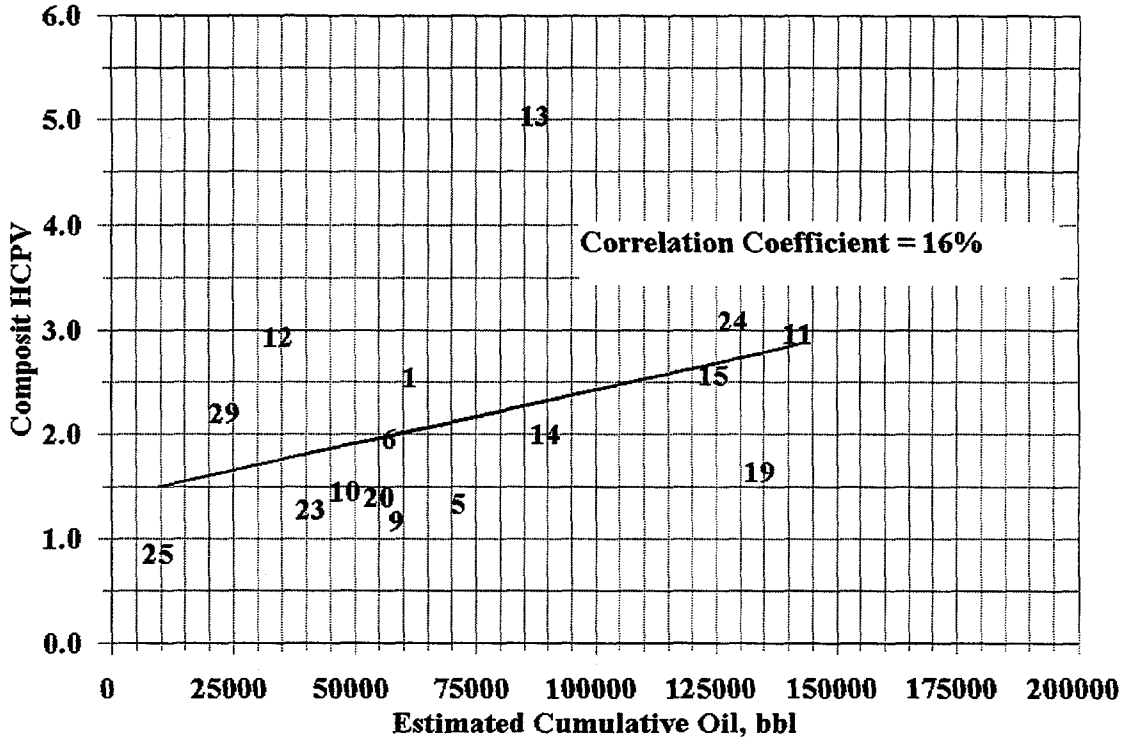

Fig. 18. Perforated zone HCPV vs. estimated cumulative oil recovery.

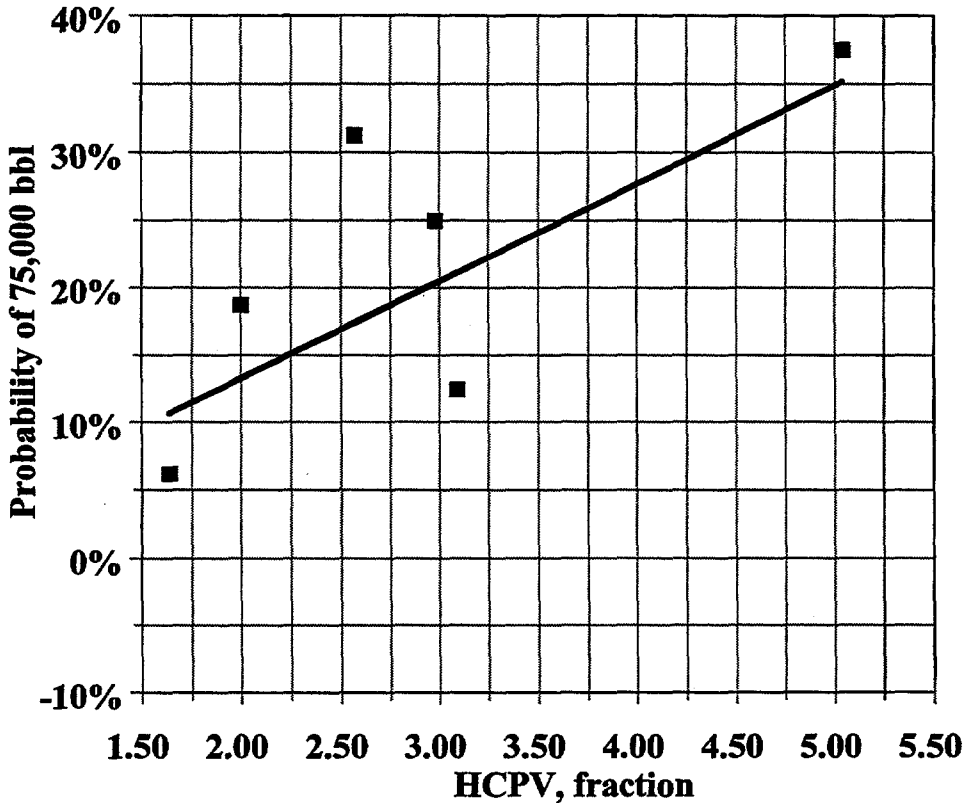

Fig. 19. Probability of a 75,000 bbl vertical well vs. HCPV.

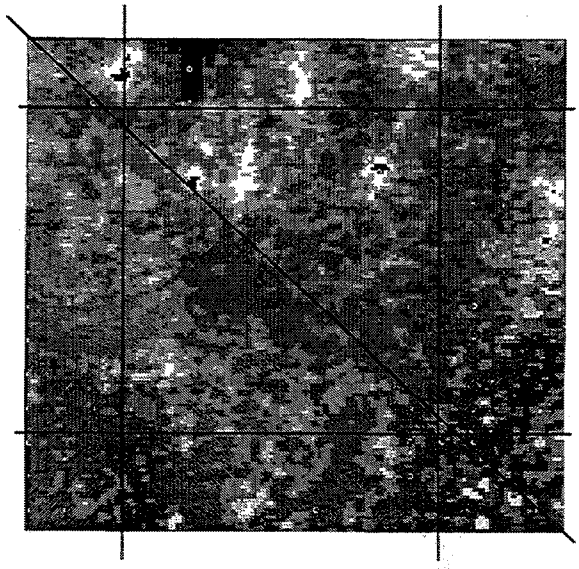

Fig. 20a. 3D seismic attributes (reference map).

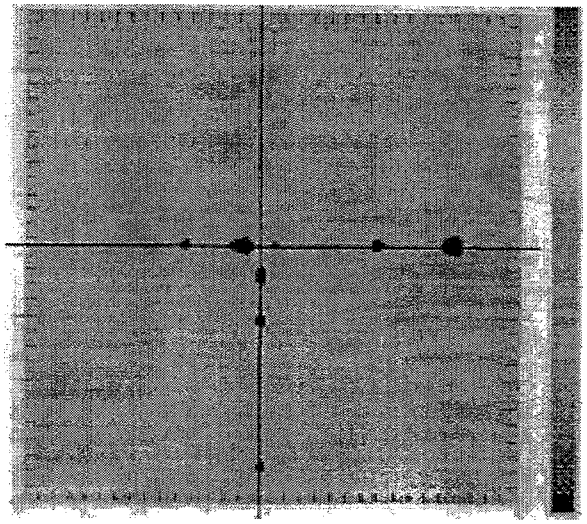

Fig. 20b. Kriged map based on two slices from reference map.

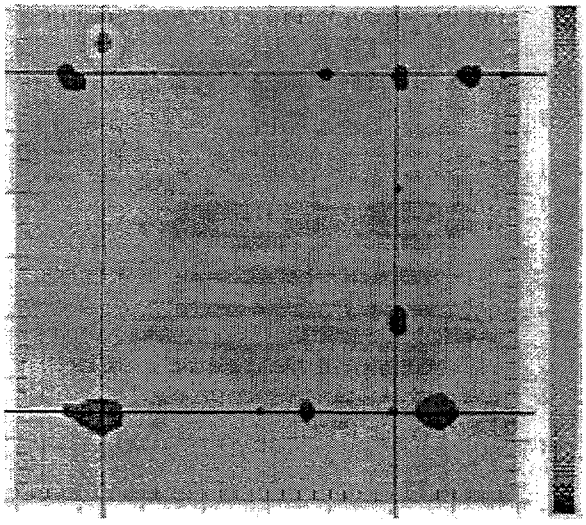

Fig. 20c. Kriged map based on four slices.

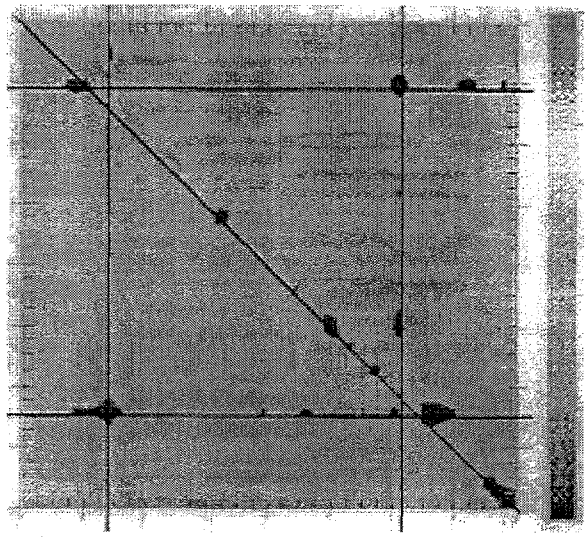

Fig. 20d. Kriged map based on five slices.

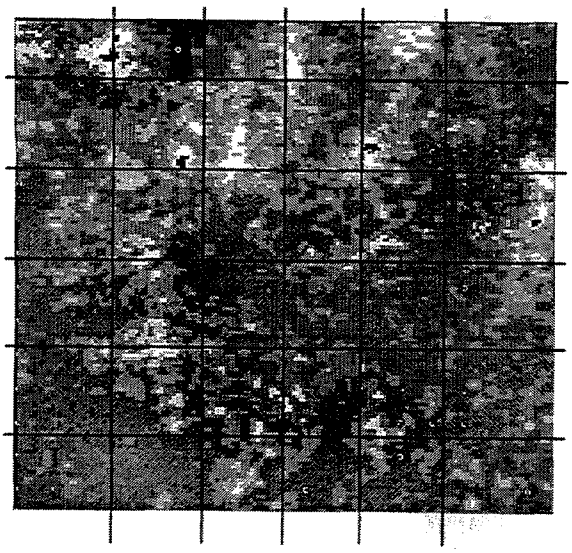

Fig. 21a. 3D seismic attributes (reference map).

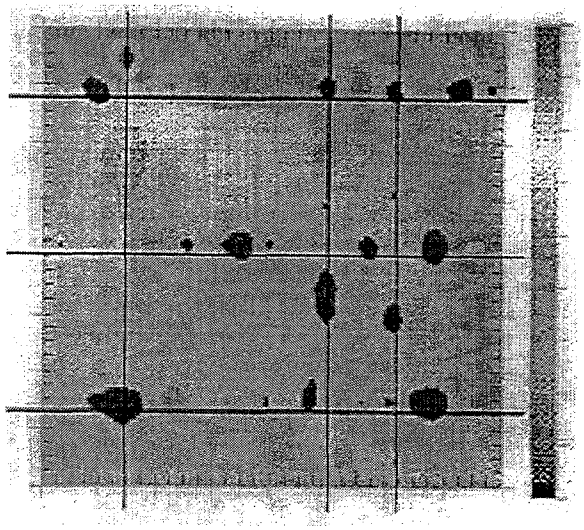

Fig. 21b. Kriged map based on five slices from reference map.

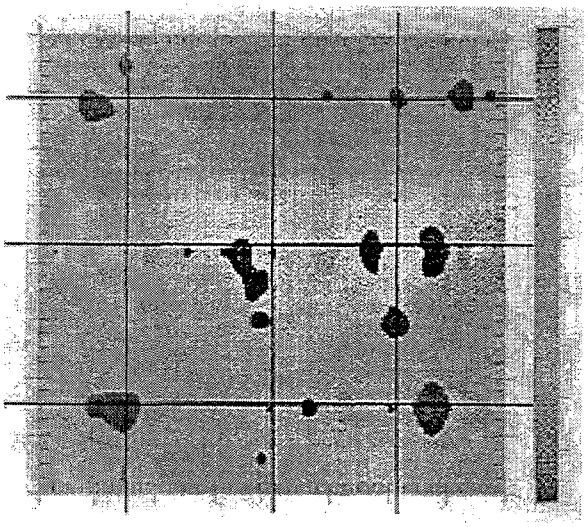

Fig. 21c. Kriged map based on six slices.

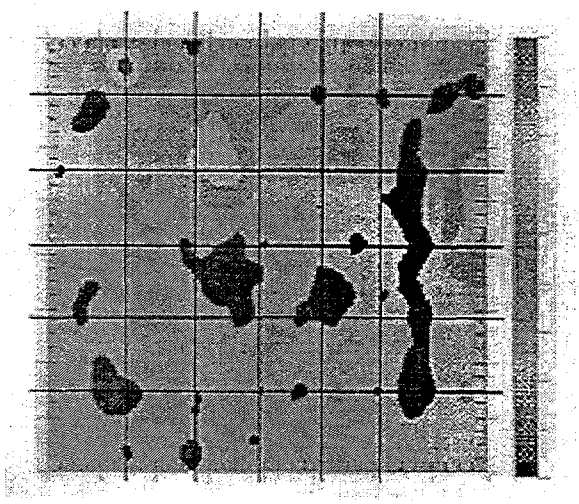

Fig. 21d. Kriged map based on 10 slices.

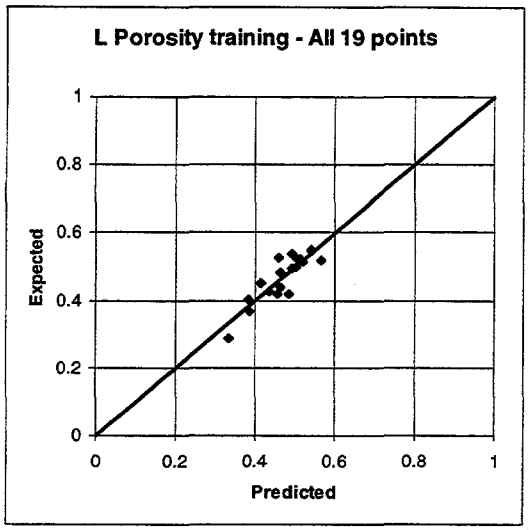

Fig. 22a

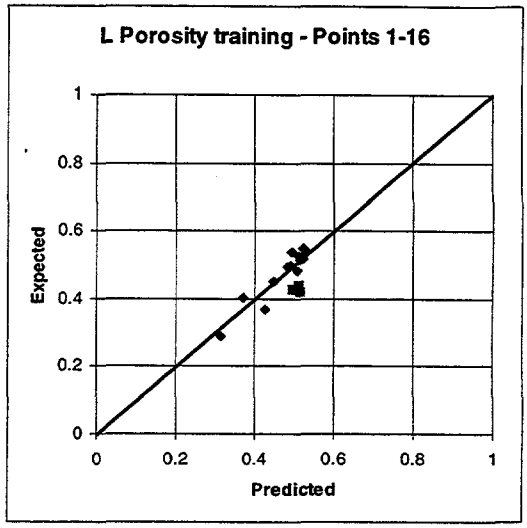

Fig. 22b

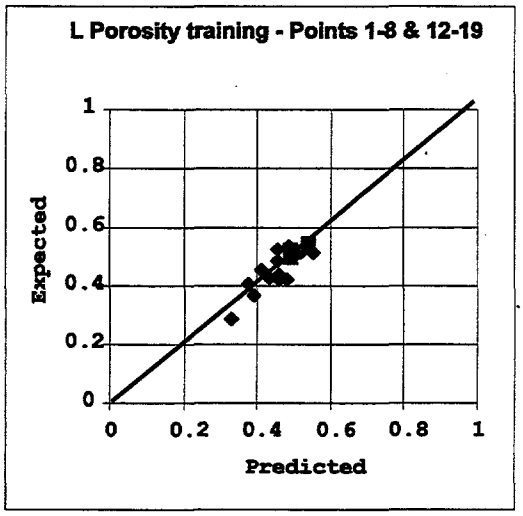

Fig. 22c

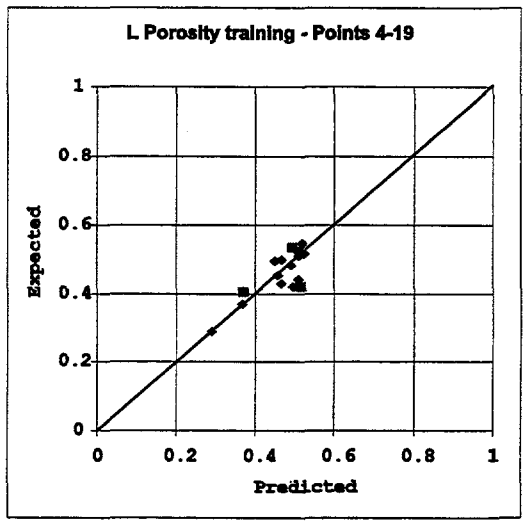

Fig. 22d

Fig. 22. Crossplots for the L-zone porosity, final and test regressions. 22a) Shows the crossplot for training with all 19 well control points. 22b) The network was retrained excluding points 17-19, which were then predicted using the network (purple points). 22c) The network was retrained excluding points 9-10, which were then predicted using the network (purple points). 22d) The network was retrained excluding points 1-3, which were then predicted by the network (purple points).

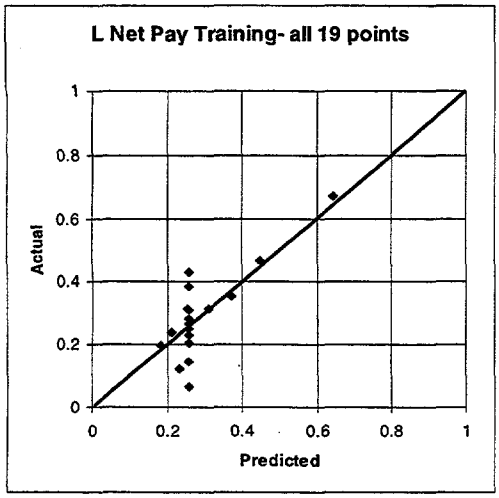

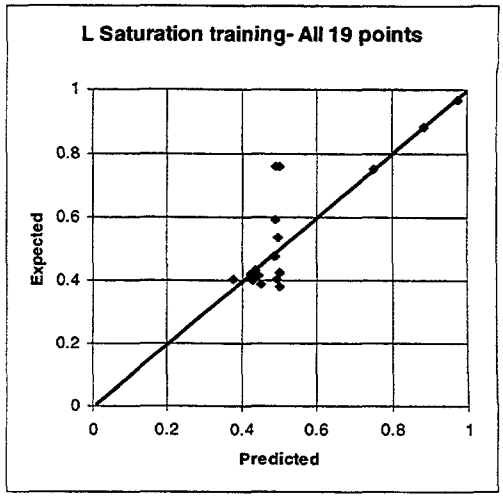

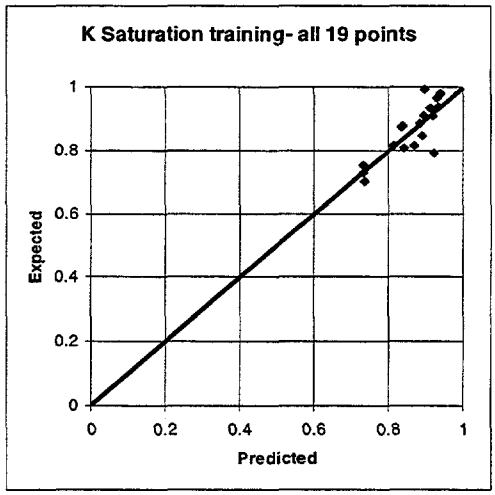

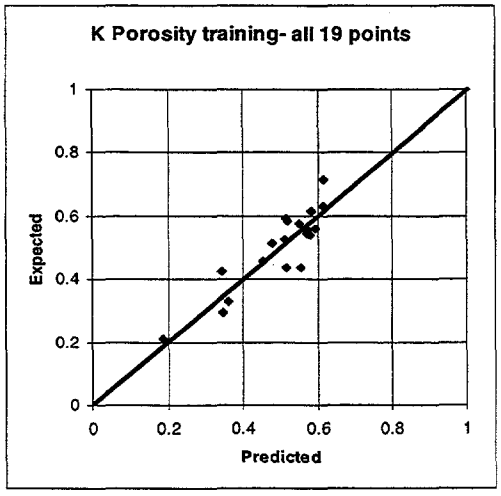

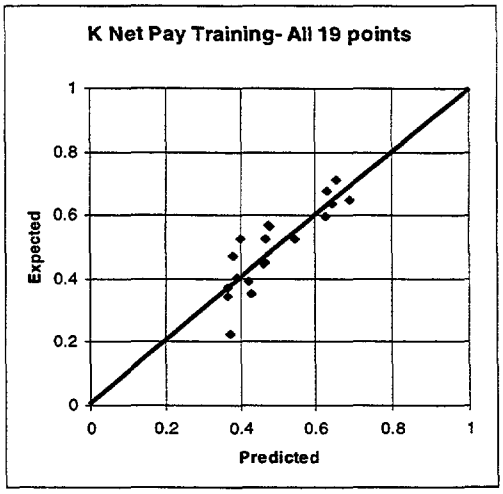

Fig. 23. Crossplots for training the L interval net pay, and water saturation; K interval porosity net pay and water saturation.

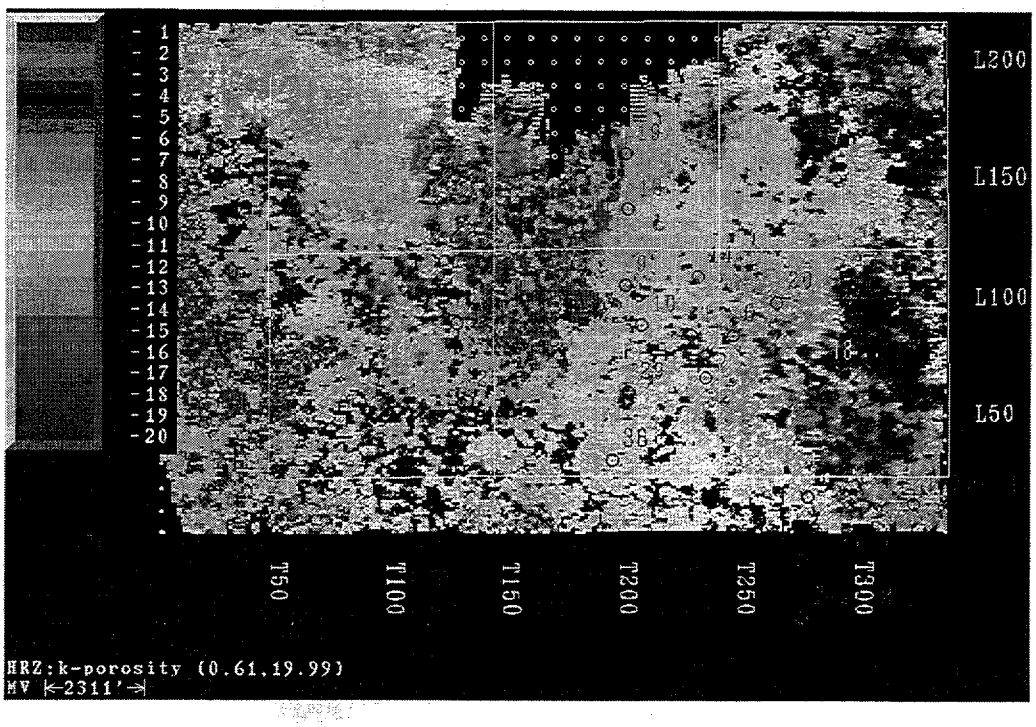

Fig 24a. Predicted K porosity.

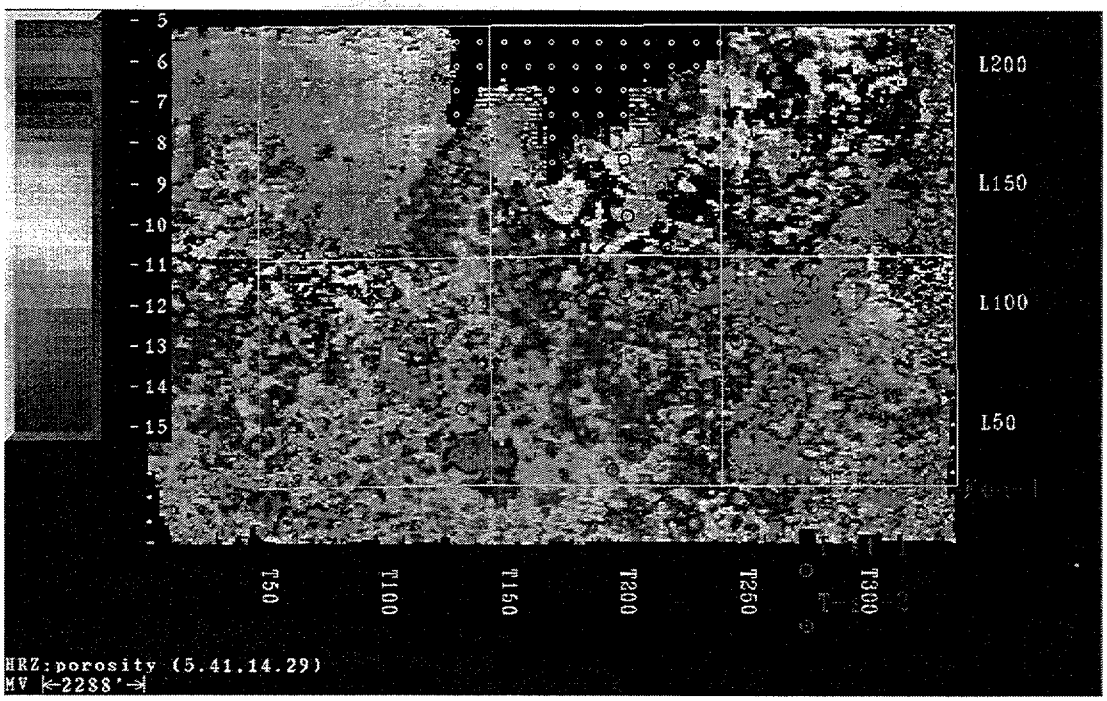

Fig. 24b. Predicted L porosity.

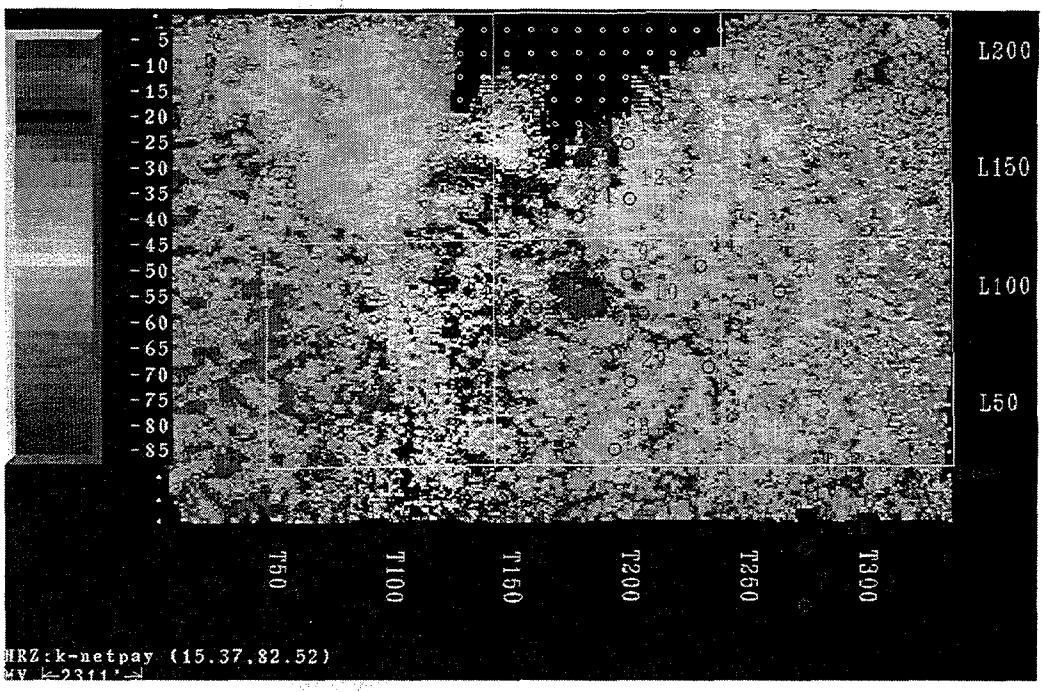

Fig. 25a. Predicted K net pay.

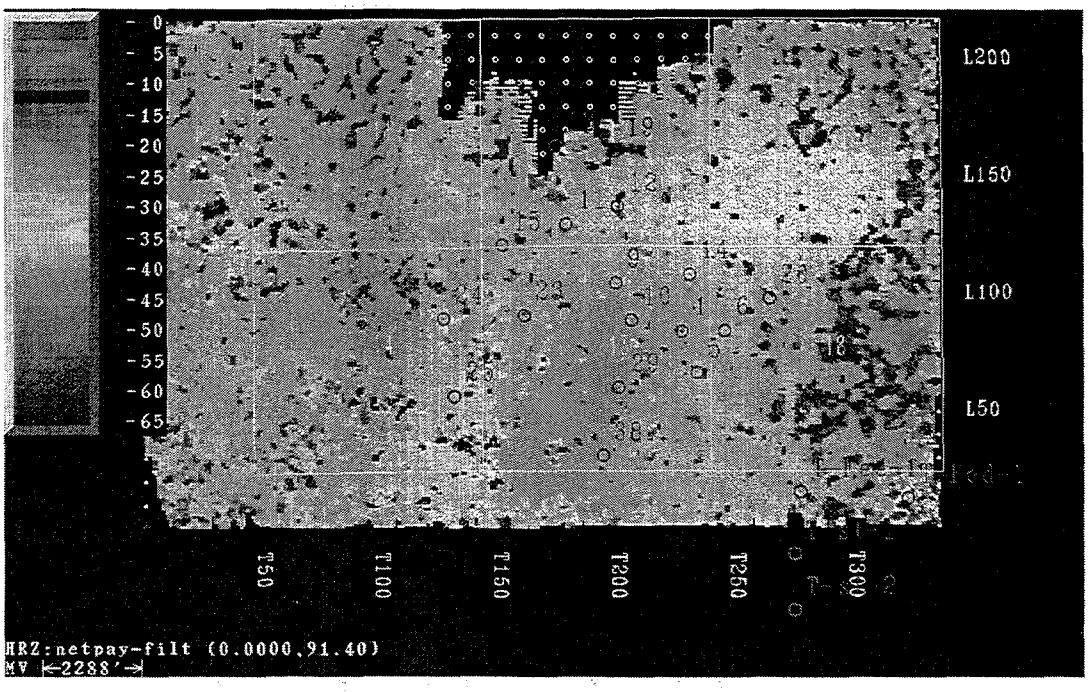

Fig. 25b. Predicted L net pay.

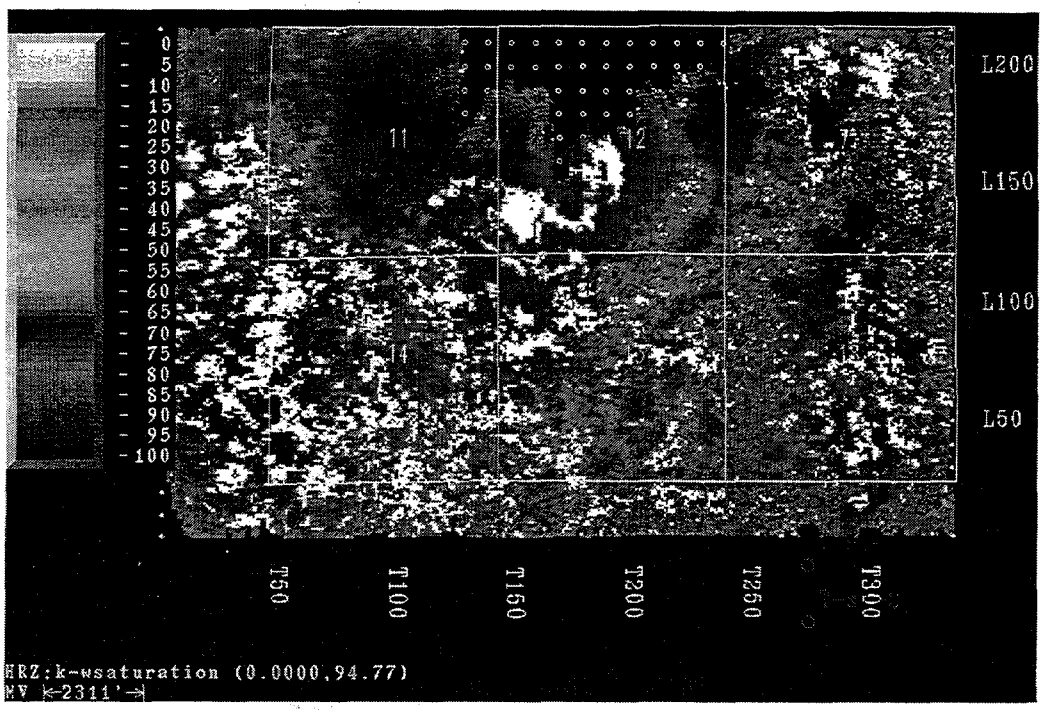

Fig. 26a. Predicted K water saturation.

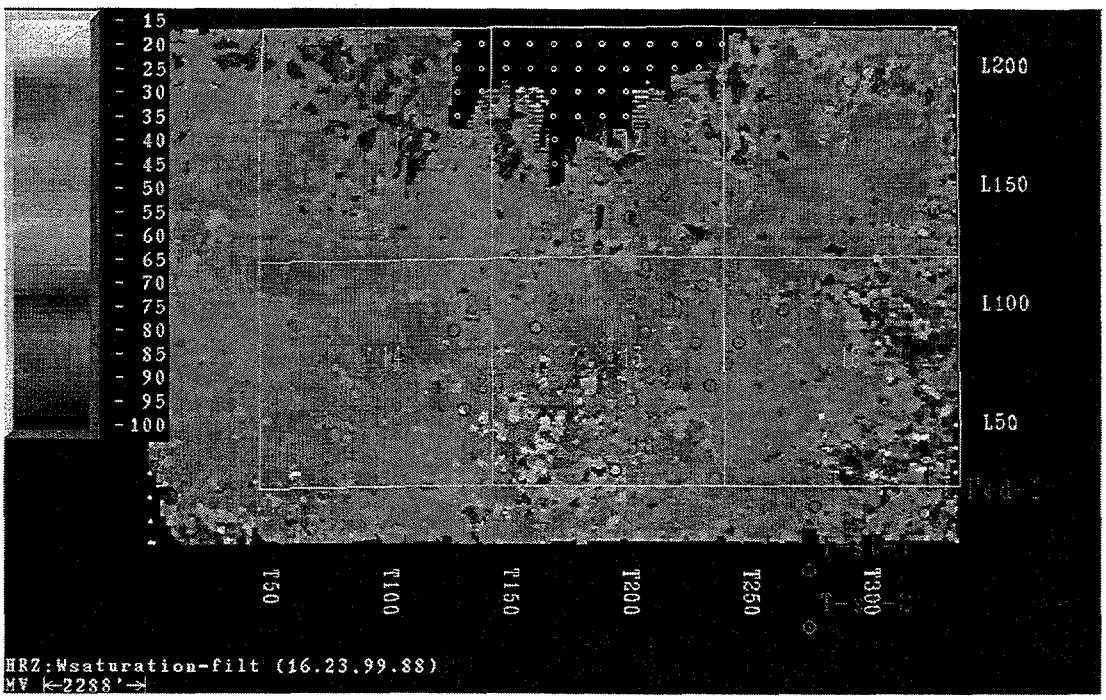

Fig. 26b. Predicted L water saturation.

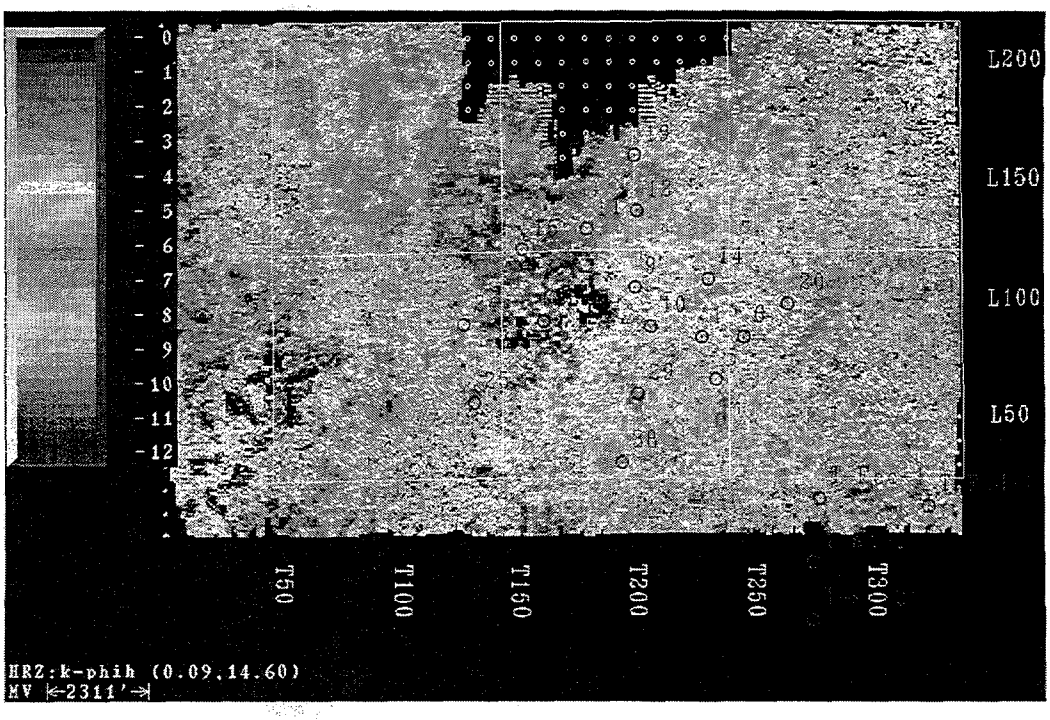

Fig. 27a. Predicted K porosity-thickness.

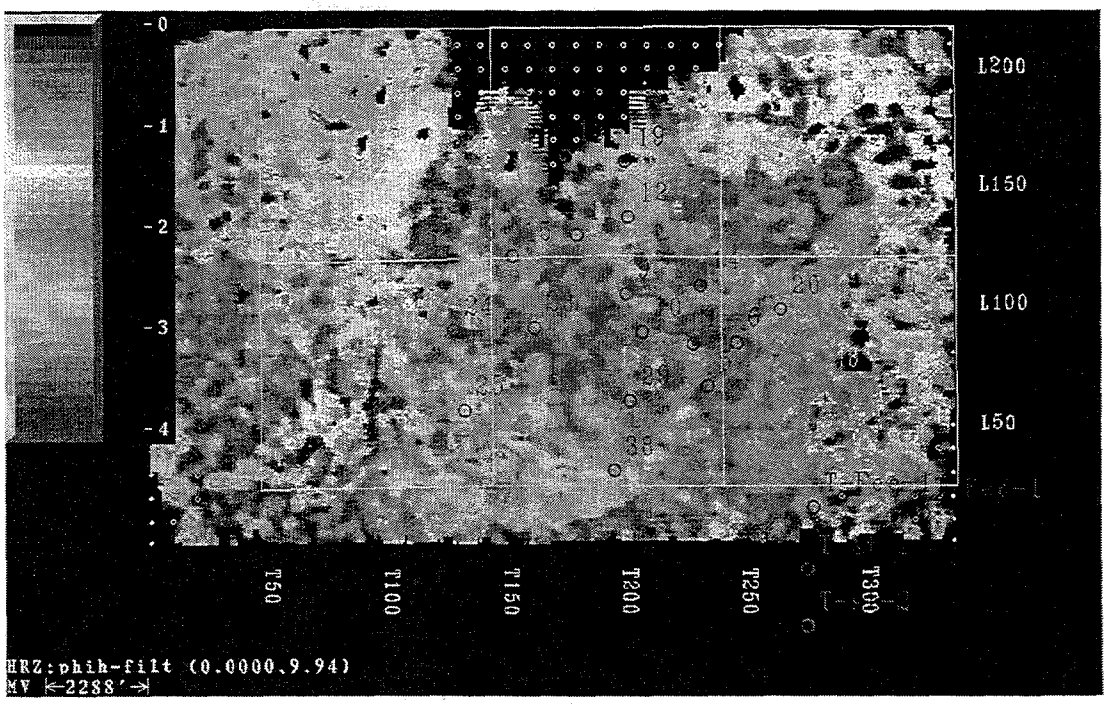

Fig. 27b. Predicted L porosity-thickness.

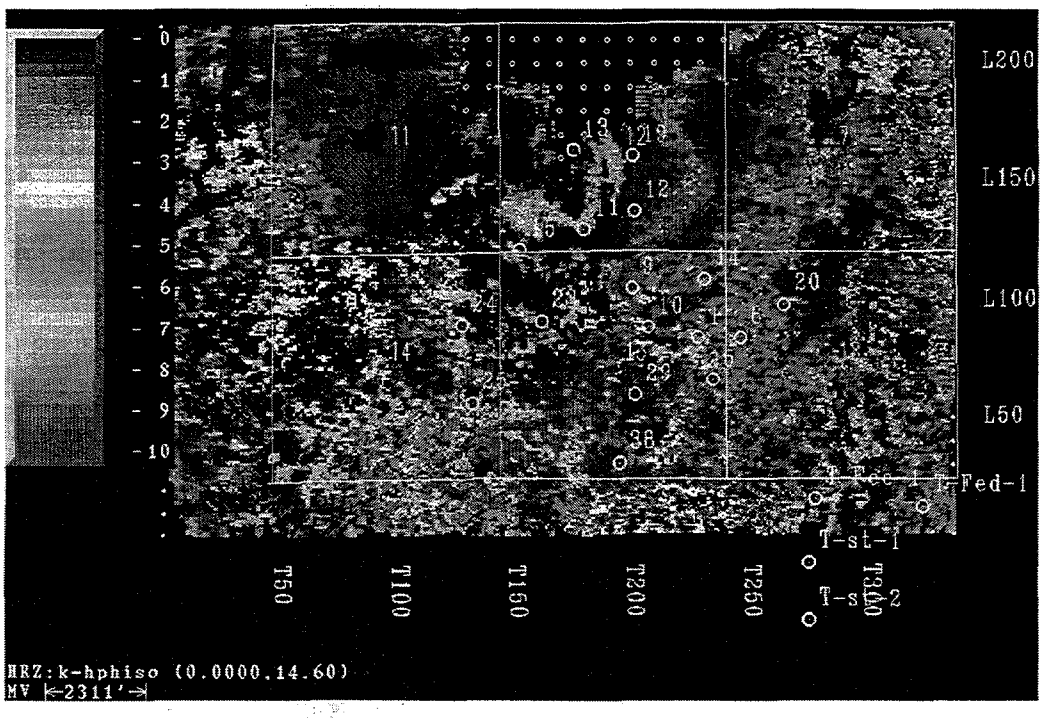

Fig. 28a. Predicted K hydrocarbon pore volume.

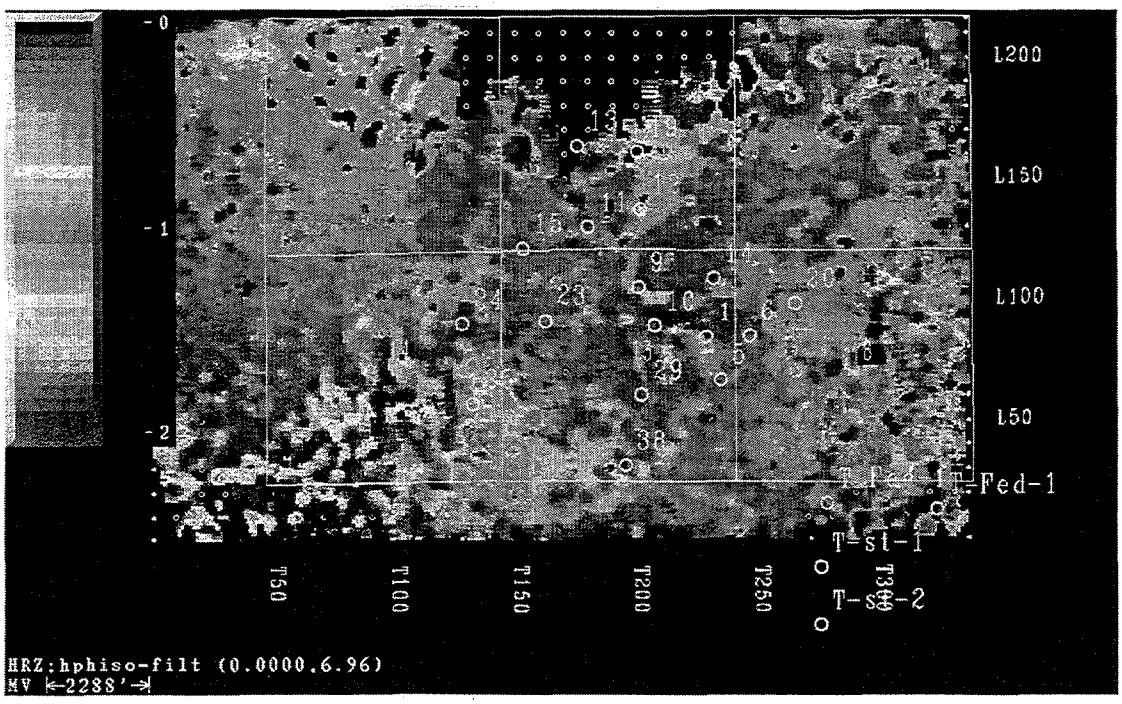

Fig. 28b. Predicted L hydrocarbon pore volume.

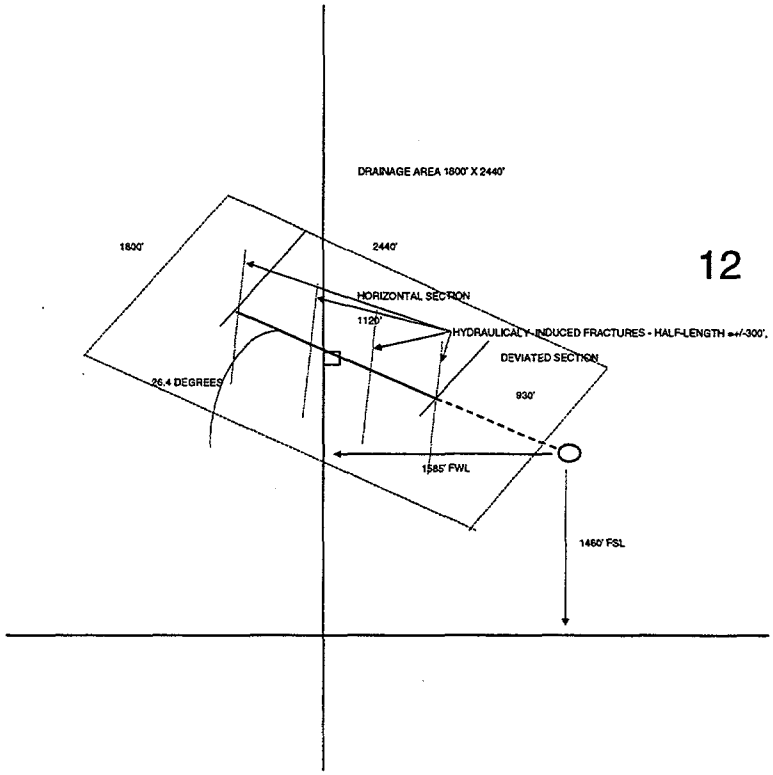

Fig. 29. Location of the planned horizontal well, NDP #36, to be located in Sections 11 and 12.